NARSIS

New Approach to Reactor Safety ImprovementS

WP3: Integration and Safety Analysis

D3.4 - Description of the approach for integration of individual subnetworks and risk interdependency

This project has received funding from the Euratom research and training programme 2014-2018 under Grant Agreement No. 755439.

Project Acronym:	NARSIS
Project Title:	New Approach to Reactor Safety Improvements
Deliverable:	D3.4 - Description of the approach for integration of individual subnetworks and risk interdependency
Month due:	M51 **Month delivered:** M54
Leading Partner:	Delft University of Technology
Version:	Final

Primary Authors: Varenya Kumar D. MOHAN, Philip J. VARDON (TU Delft)

Deliverable Review:

- **Reviewer #1:** Andrej Prošek, JSI **Date:** 25/02/2022
- **Reviewer #2:** Jeremy Rohmer, BRGM **Date:** 25/02/2022

Dissemination Level		
PU	Public	**X**
PP	Restricted to other programme participants (including the Commission Services)	
RE	Restricted to a group specified by the consortium (including the Commission Services)	
CO	Confidential, only for members of the consortium (including the Commission Services)	

Table of contents

List of Figures

List of Tables

List of Abbreviations

BN	Bayesian Network
BN-SLIM	Bayesian network-success likelihood index method
CCF	common cause failure
CDF	cumulative distribution function
CPT	conditional probability table
EDG	emergency diesel generator
EDP	engineering demand parameter
EFWS	emergency feedwater system
ESD	event sequence diagram
HEP	human error probability
I&C	instrumentation & control
IDA	Information, decision, action
IM	intensity measure
JPD	joint probability distribution
kV	kilo volt
LOOP	loss of off-site power
MWe	Megawatts electric
NPP	nuclear power plant
OOBN	object-oriented Bayesian network
PCD	partial cool down
PDF	probability density function
PGA	peak ground acceleration
PSA	probabilistic safety assessment
PSF	performance shaping factor
RFEM	random finite element method
RHR	residual heat removal
SBO	station blackout
SCD	secondary cool down
SLIM	success likelihood index model
SSCs	systems, structures and components
US NRC	United States Nuclear Regulatory Commission
VPP	virtual power plant
WP	work package

1 Executive Summary

A generic, step-wise, iterative methodology for multi-risk integration using Bayesian networks (BNs) is proposed. The method relies on the predictive capabilities of the BN to estimate top and intermediate event probabilities and uses its diagnostic inference abilities to analyse sensitivity and improve network efficiency. The BN-based risk methodology was applied to the project accident scenario at a virtual nuclear power plant (NPP) developed within Work Package 4 of the NARSIS project. The accident scenario involves an external hazard event-related loss of offsite power that leads to a station blackout event and eventually to failure of the secondary cool-down system. Earthquake and flooding hazards, along with their interactions, were considered in the risk analysis. The interaction of these hazards with the subnetworks developed in deliverable D3.2 (Mohan et al., 2021) was modelled using the BN methodology. Subnetworks modelling the following aspects were integrated:

(i) Station blackout under loss of offsite power
(ii) Failure of the secondary cool down system following station blackout
(iii) Geotechnical reliability of a flood control dike
(iv) Human error probability estimation for an operator action during event progression from station blackout to failure of the secondary cool down system

The integration of hazards with subnetworks was performed in two ways. The first method is an object-oriented BN (OOBN) approach where basic fault trees (FTs) and hazard trees in existing probabilistic safety assessment (PSA), can be individually converted to BNs - risk objects. These separate risk objects are integrated by defining their interactions as per the associated event trees (ETs). In the second approach, a unified BN is constructed by combining hazards and all subnetworks within a single BN. Both these approaches were demonstrated using the station blackout subnetwork. The OOBN approach allows for an exact, parallel conversion of ETs and FTs, as in the existing PSA. While predictive and diagnostic inference are possible within risk objects, only predictive inference is possible across risk objects. The unified BN allows for both predictive and diagnostic inference between the top event and all subnetworks. However, the unified BN can prove to be computationally more demanding than the OOBN approach. For the project accident scenario, the unified BN approach resulted in a 1 to 2 orders of magnitude increase in run time and a linear increase in memory used, as compared to any of the individual subnetworks.

A unified BN was built to integrate multiple hazards with the aforementioned subnetworks. The unified network indicated a relatively low probability of a hazard-induced accident. However, if the hazard events were to occur, they would significantly increase the chance of an accident. Using a unified BN approach allowed for interaction of the subnetworks with the hazards as well as with each other. Diagnostic analysis of the influence of dike failure mechanisms on the top event occurrence were possible due to the representation of advanced numerical models of flood defence reliability as BN-based surrogate models. Similarly, the integration of a BN-based human reliability subnetwork allowed to assess the influence of human performance shaping factors on the probability of top event occurrence.

The use of BNs in a multi-risk integration methodology provide several advantages including the accurate modelling of dependencies between hazards. Such unified BNs also allow the identification of dependencies between top events and the parameters driving fragilities of systems, structures and components (SSCs), which may not be normally be considered in design. However, modelling the interaction of multi-hazards with several SSCs in a single BN can result in a computationally intensive BN that is difficult to decipher visually.

While system-level implementation of BNs is valuable and relatively easy, plant-level implementation can also be possible with a judicious approach to BN application. All the ET/FTs at an NPP may be converted to risk objects using the OOBN approach, to firstly reproduce the results of existing PSA. Subnetworks may be integrated using unified BNs when deemed necessary. While this may not represent a complete solution that models every known dependence in the NPP, BNs can still complement and improve existing PSA results.

2 Introduction

One of the key objectives of the NARSIS project is to improve the integration of external hazards and their consequences using state-of-the-art risk assessment methodologies. Within NARSIS Work Package 3 (WP3), Deliverable D3.1 (Mohan et al., 2018) presented a review of various risk integration methods and identified Bayesian networks (BNs) as a suitable framework for considering external hazards and consequences. Deliverable D3.2 (Mohan et al., 2021) presented the methodology and examples of the development of individual BNs (subnetworks) characterising various technical and human aspects within a nuclear power plant (NPP) during an external event related accident scenario. This deliverable (D3.4) presents the methodology and its application for integration of the above subnetworks, within a BN-based risk framework.

A simplified example accident scenario was assumed for the purpose of demonstrating subnetwork development and BN use in the context of NPP risk assessments. It is noteworthy that the accident scenario or associated subnetworks may not be completely representative of any real NPP or the various systems, structures and components (SSCs). The plant design details or event progressions are details that are of lower importance for this study.

A comprehensive multi-risk integration methodology, using BNs, is presented. For the chosen accident scenario, the subnetworks developed in D3.2 (Mohan et al., 2021) are integrated using this BN-based method.

2.1 Multi-risk integration in the nuclear industry

The safety of facilities, such as those belonging to the chemical, aviation and nuclear industries, is threatened by several hazards (Janic, 2000; Lees, 2005; US NRC, 1975). The critical feature, common to the aforementioned industries, is that the consequences from adverse events at these facilities can be catastrophic (Hopkins, 2011). A very high safety level is warranted and usually achieved, and therefore, industries such as nuclear, chemical and aviation may be termed as high reliability industries (Hofmann et al., 1995; Rausand, 2013).

Risk assessments in high reliability industries pose several challenges. Low-probability, multi-hazard combinations and their cascading effects, must be considered due to the potentially catastrophic consequences (Roberts, 1990). These facilities are generally composed of several interacting systems, and accounting for these interactions makes them complex to analyse. Moreover, there are very few cases of significant accidents in these industries, which precludes conventional statistical analysis to predict future risks (Leveson et al., 2009). Probability estimates of various hazards and their impact to SSCs, are also subject to uncertainty. Thus, high reliability industries require a multi-risk integration framework that considers even low-probability external hazard events. The risk framework should account for the impact of these hazards on complex, dependent systems, and also allow for inclusion of expert judgement where data is sparse. The risk framework must also be suitable for tracking uncertainties in the data and propagating them to the final risk estimate.

Multi-risk assessment involves the consideration of not only different hazards but also their interactions with other hazards (Mignan et al., 2014; van Erp and van Gelder, 2015). Interactions between hazards happen in two ways: (i) hazards may independently occur within a short time window, or (ii) the occurrence of one hazard may have cascading effects that lead to one or more other hazards. The impact on SSCs from hazards, i.e. their fragilities, can be classified into two types: (i) the SSCs are impacted by multiple hazards at the same time or, (ii) multiple hazards affect the SSCs at different times, progressively damaging them over time. Further, different intensity measures (IMs, or loading types) of the same hazard can also affect SSCs differently (Gehl et al., 2013). For instance, the peak ground acceleration (PGA) and the spectral acceleration at a period of 0.5 s of an earthquake event, may have different effects on the same structure. Vector-based fragility models have been shown to perform better than single-IM fragility curves, in multi-hazard scenarios where SSCs are sensitive to different IMs

(Gehl and Rohmer, 2018). Given such a wide variety of hazards and SSCs, it is also important to identify which hazards and fragilities contribute most to the risk. This enables efficient allocation of resources towards advanced hazard and fragility analyses that could reduce the uncertainty in risk estimates.

Another aspect of multi-risk assessments is the consideration of risk from human error. Current methods often rely on the separate calculation of human error, and their integration with the overall risk assessment framework for the NPP becomes challenging. In this regard, several improvements have been proposed (Ale et al., 2006; Kazemi et al., 2017; Mohaghegh et al., 2009). Nevertheless, this study aims to improve the integration of human factors with the overall risk framework, while also handling aforementioned challenges such as hazard dependence, vector-based fragility and expert judgement integration.

3 Bayesian network-based risk integration framework

This study presents an integrated risk framework that can meet the aforementioned requirements for high reliability industries. BNs are used for risk integration to account for dependencies between hazards and their interaction with SSCs. Sensitivity analysis in the network allows the elimination of hazards and dependencies with negligible impacts on the calculated risk. Bayesian inference within the network is used to identify critical ranges of hazards and fragilities, enabling focused secondary analyses that can improve overall risk estimates. Thus, the BN would act both as a screening tool and as an overall risk integration framework.

3.1 Bayesian networks

A BN is a specific application of Bayesian probability theory. It is a directed acyclic graph, composed of 'nodes' that correspond to random variables and 'arcs' that link dependent variables. The directions of the arcs indicate the dependencies between the nodes (i.e. directed), and these arcs never cycle back from the child nodes to the parent nodes (i.e. acyclic). Hence, the network is a visually explicit representation of the mutual relationship between random variables, and represents the joint probability distribution (JPD) of all random variables within the model (Koller and Friedman, 2009). A simple example is shown in Figure 1. The random variables in the network may be represented by discrete or continuous probability distributions.

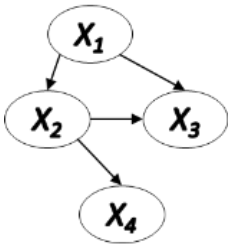

Figure 1: Example of a Bayesian network; X_i indicates a random variable.

The dependencies between random variables are usually encapsulated within conditional probability distributions (given by ($\mathrm{P}(X_i|Parents(X_i))$, where P indicates probability and | indicates conditionality) at each node. The JPD is given by the chain rule of BNs:

$$\mathrm{P}(X_1, X_2, \dots, X_n) = \prod_{i=1}^{n} \mathrm{P}(X_i \,|Parents(X_i)) \qquad \text{Eq. (1)}$$

The JPD of the example in Figure 1 is given by:

$$\mathrm{P}(X_1, X_2, X_3, X_4) = \mathrm{P}(X_1)P(X_2|\, X_1)P(X_3|X_1, X_2)\mathrm{P}(X_4|\, X_2) \qquad \text{Eq. (2)}$$

The JPD can be queried to infer the state of a random variable, given our beliefs regarding the other variables, via Bayesian inference. In other words, BNs can be used to answer probabilistic queries in a multivariate problem when one or more variables have been observed. The types of inference algorithms and other characteristics, advantages and challenges associated with BNs are discussed in detail in D3.2 (Mohan et al., 2021).

3.2 The risk integration methodology

The methodology proposed in this study consists of a series of five steps in which a risk integration BN is constructed and calculations are run using it. These steps are consecutively implemented in two stages - Levels I and II. Figure 2 presents the outline of the methodology.

Level I Integration

The objective of Level I integration is to assess the impact of various hazards and damage states of SSCs, on the probability of the adverse end event. During Level I, it is possible to assume regional hazard curves and/or generic fragility models (based on similar components) that are not necessarily site-specific. At the end of Level I integration:

(i) inconsequential nodes (random variables associated with hazards) and arcs (dependencies between hazards or IMs) are identified from sensitivity analyses

(ii) critical ranges of hazards and damage states are determined through diagnostic inference in the BN

These results are transferred to Step 1 of Level II Integration, where the steps 1-5 are repeated in the light of results from Level I.

The following five steps are implemented sequentially in each of Level I and II, as shown in Figure 2:

Step 1 – Single and multi-hazard analysis, event sequence definition, and fragility modelling:

(i) A list of relevant hazards is selected based on historic events at the industrial facility of interest. Hazard curves for the return period(s) of interest are calculated for all hazards, either from regional data or site-specific information, if available.

(ii) Based on the approaches prescribed in Liu et al. (2015), feasible hazard interactions and cascades are identified. These can also be theorised based on the site location. Conditional probability distributions are determined in the case of dependent intensity measures (IMs), concurrent hazards and cascading hazards.

(iii) The adverse top event of interest is known and the corresponding event sequence is determined, either logically by experts or by using existing PSA information such as event trees and fault trees.

(iv) Based on the event sequence, the list of SSCs involved are determined. The event sequence is used to ascertain dependence between random variables in the risk analysis – hazards, damage states of SSCs and consequential events in the industrial facility.

(v) For every pairwise combination of a hazard and an SSC, fragility models are developed or obtained from literature, including vector-based fragilities considering multiple IMs.

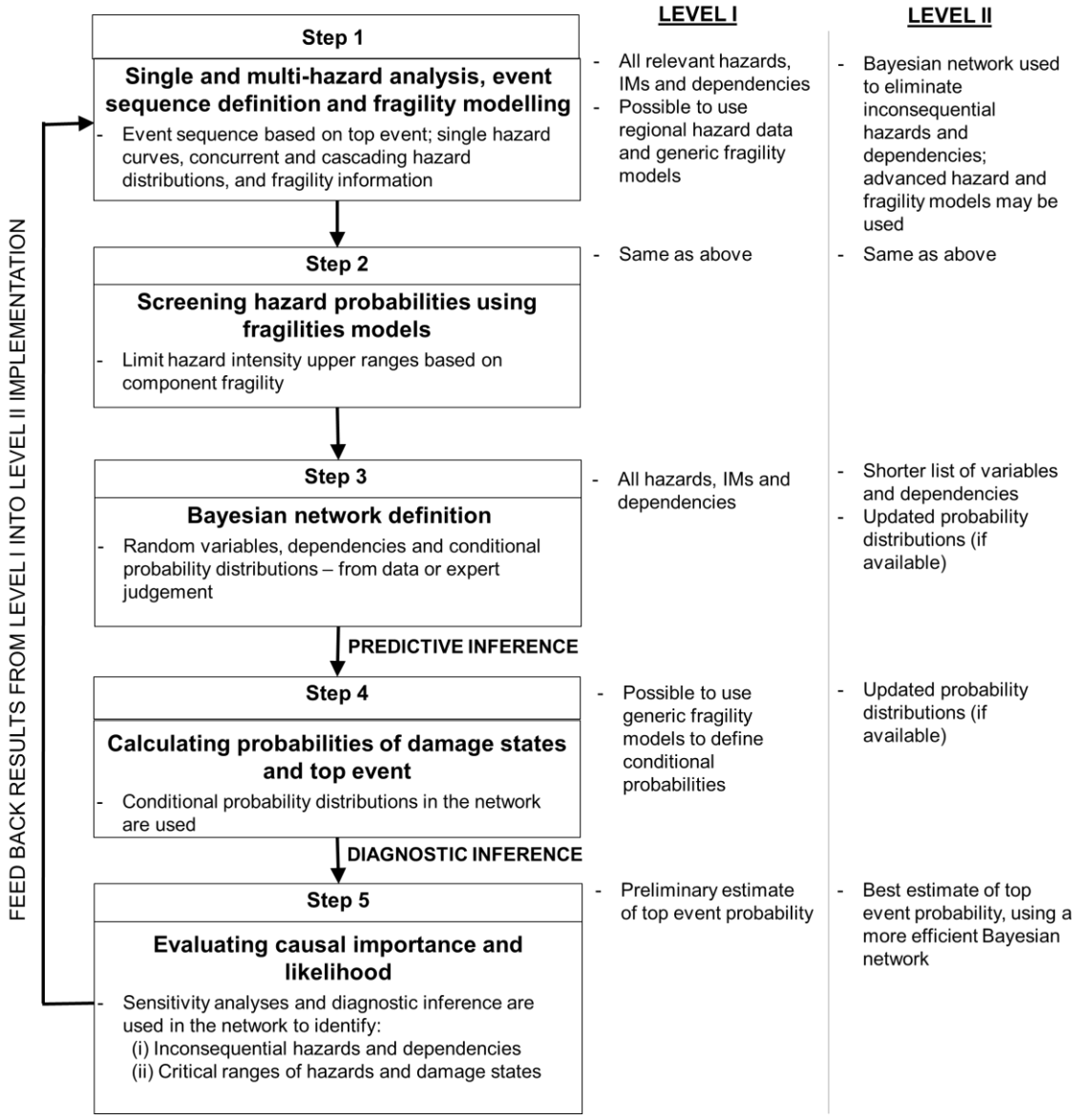

Figure 2: Step-wise multi-risk integration methodology using Bayesian networks

Step 2 – Screening hazard probabilities using fragility models

The objective of this step is to identify the relevant ranges of hazard magnitudes that would affect various SSC. Each of the selected hazards is assessed against the corresponding fragility model of every SSC, independently. For a given hazard, the lowest hazard magnitude that triggers damage amidst all SSCs is chosen to determine the lower bound of that hazard curve (threshold value of damage is of interest here). Hence, refined probability distributions across the relevant range of magnitudes, are available for the occurrence of each hazard or hazard combination.

Step 3 – Bayesian network definition

The selected hazards, damage states and consequential events in the facility are chosen as the (random) variables of interest and comprise the nodes of the BN. The arcs of the BN are defined by the chosen hazard interactions, accident event sequence and/or expert judgement, where required. If the accident sequence is derived from existing PSA information such as event trees and fault trees, these can be directly converted to a BN based on (Bobbio et al., 2001). Such event and fault trees are usually composed of system events within the facility, and external hazard events are not explicitly included. Accordingly, if the BN is obtained from conversion of fault trees, only hazards and their dependence with SSCs need to be additionally defined in the BN.

The conditional dependence between variables involved is known from the fragility models, event sequence (for e.g. fault tree logic gates) and/or expert judgement, where required. Expert judgement may be used to define conditional probability relations based on Cooke (1991). The application of this method to various industries has been reviewed by Cooke and Goossens (2008). Thus, at the end of Step 3, the entire structure of the BN is available with nodes (random variables in the risk analysis), arcs (directional dependence between random variables) and associated marginal or conditional probability distributions at each node.

Step 4 – Calculating probabilities of damage states and adverse end event

Predictive inference in the BN is used to calculate the probability of damage states, using the conditional probability distributions. For different hazard levels or damage states, the probability of the top event is also calculated in the BN.

Step 5 – Evaluating causal importance and likelihood

Sensitivity analyses are performed in the BN, to identify hazards that have negligible impact on the probability of occurrence of the top event. Similarly, the impact of dependencies between different hazards or between IMs of the same hazard can be assessed. Further, diagnostic inference is used; i.e. the top event is assumed to have occurred and the posterior probability distributions of hazards and damage states are calculated. This provides the range of hazards and damage states that are most likely to cause the top event.

Level II Integration

The objective of Level II integration is to thoroughly investigate impactful hazards and fragilities, and arrive at the end event probability using a more efficient BN. In this level, inconsequential hazards and dependencies, determined in Level I, are removed from consideration. During Step 1 of this level, site-specific analyses for specific hazards (single and multi-hazards) of interest may be performed, if not included in Level I. Fragility analyses can be performed for specific SSCs for these hazards or combinations, focusing on the critical range of hazards and damage states determined in Level I. Results from these targeted, site-specific analyses can be incorporated into the BN in Step 3. If no further improvements are possible or necessary, on the hazard and fragility data used in Level I, the BN in Level II is still computationally more efficient because inconsequential hazards and dependencies have been removed. Steps 4 and 5 are implemented as before.

Hence, at the end of Level II, the BN has been filtered to its most efficient structure, with the most relevant data and provides the best estimate for probability of occurrence of the top event at the NPP. Any new information, if made available, can be similarly included in subsequent levels, producing updated probabilities for the top event.

It is important to note that some of these steps and/or iterations can happen out of sequence or simultaneously. For e.g. the filtering of inconsequential hazards can already happen in a dedicated multi-hazard analysis (as in NARSIS WP1), without the use of the BN. This framework is only a guide to the different steps involved in building a BN-based multi-risk model.

3.3 Some potential challenges and solutions

Multi-hazard integration with BNs can present several challenges. Here we look at two expected difficulties and their respective solutions. Converting large event and fault trees to BNs (in *Step 3* of the above methodology) can result in large discrete BNs. The computational demands of these BNs are still usually not a problem as the fault trees are only a specific case of the BN and implement the same logic. However, when hazard nodes are added to the BN and several subnetworks are combined together, the computational demands can rise significantly.

3.3.1 Discretised distributions

Hazard events given by detailed probability distributions, spanning a wide range of their intensity measure(s). The use of the dynamic discretisation algorithm in AgenaRisk® allows for the relatively easy use of continuous variables (Neil et al., 2007). However, it is rare to fit parametric continuous distributions to hazard nodes and hence, hazard distributions are often discretised. The challenges associated with using continuous and discretised variables are discussed in detail in D3.2 (Mohan et al., 2021). Discretising these distributions for risk integration can result in large discrete BNs with significant computational demands.

The *Noisy-OR* is an assumption that is useful in simplifying large discrete BNs, allowing the number of conditional probability table (CPT) entries to grow linearly with the number of parents (Pearl, 1988). This concept is most easily exemplified by the binary Noisy-OR gate. Let $X_1, \dots X_i, \dots, X_n$ be n binary parents of Y, where:

(i) each of X_i has a probability p_i of being sufficient to cause Y to be true, when all other parents are false, and
(ii) the probability of each parent being true is independent of the states of the other parents.

The above two assumptions enable the specification of the conditional probability distribution of Y using only n probabilities, $p_1, \dots p_i, \dots, p_n$. p_i can be expressed as:

$$p_i = \mathrm{P}(y \mid x_1', \dots x_i, \dots, x_n') \quad \text{Eq. (3)}$$

Where x_i' is the complement of x_i.

Given any X_p belonging to the X_i's that are true, the following applies:

$$\mathrm{P}(y \mid X_p) = 1 - \prod_{i:X_i \in X_p} (1 - p_i) \quad \text{Eq. (4)}$$

With just the above equation, the complete CPT for the child node Y can be derived, given any X_p.

The next step to the Noisy-OR assumption is the *leaky Noisy-OR* gate, where the child variable may be true even if all of its parents are false. In other words, all the causes of Y are not explicitly known and there are unknown reasons for Y to be true. The probability that Y can occur despite the explicit causes being false may be termed as the leak probability, p_0 given by:

$$p_0 = \mathrm{P}(y \mid x_1', \dots, x_n') \quad \text{Eq. (5)}$$

In the leaky Noisy-OR assumption, p_i ($i \neq 0$) is the probability that Y is true when X_i is true (not necessary that X_i being true causes Y to be true) and all other parents are false. Let p_i' be the probability that Y is true when X_i is true, when all other parents are false and unmodelled causes are also absent (i.e. X_i being true causes Y to be true). This implies:

$$1 - p_i' = \frac{1 - p_i}{1 - p_0} \quad \text{Eq. (6)}$$

Now, in the case of the leaky Noisy-OR, given any X_p belonging to the X_i's that are true, the following applies:

$$\mathrm{P}(y \mid X_p) = 1 - (1 - p_0) \prod_{i:X_i \in X_p} \frac{1 - p_i}{1 - p_0} \quad \text{Eq. (7)}$$

Hence, with the above equation, the complete CPT for the child node Y can be derived, given any X_p. Another way of expressing the Noisy-OR concept, is using the concept of an *inhibitor*. For any i, if X_i is true then Y is true with a certain probability unless a preventing factor – the inhibitor – prevents it with probability z_i. All such inhibitors are assumed to be independent.

The Noisy-OR is a particular case of a more general concept called divorcing. Consider the BNs in Figure 3a, with parents *a1, a2, a3* and *a4* and child variable *b*. This BN can be modified to an equivalent BN by introducing an intermediary variable *c* as shown in Figure 3b. While the first BN, will require 2^4 entries for the CPT of b, the second BN will need a total of $2^2 + 2^3$ ($< 2^4$) CPT entries at nodes *c* and *b*. This is called divorcing.

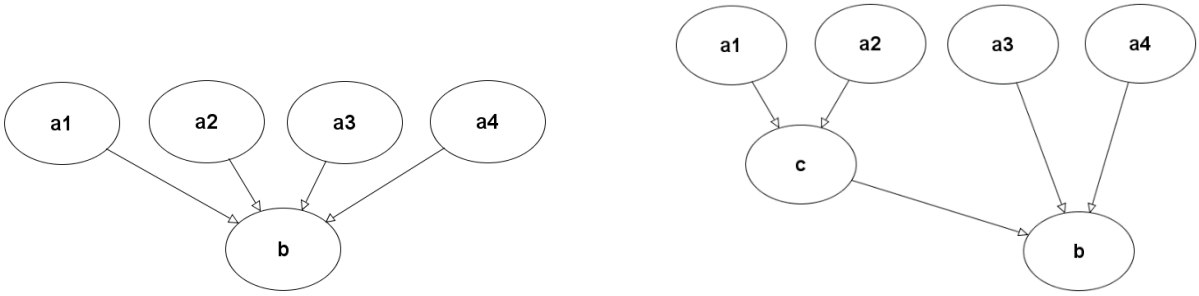

Figure 3: (a) Example network for divorcing; (b) nodes a1 and a2 are divorced from a3 and a4 using c

3.3.2 Damage state calculation using fragility functions

When the hazard distributions are discretised, the CPTs at component damage state nodes, calculated using fragility functions, can become large. Despite simplifications such as the Noisy OR, building CPTs for complex problems be unwieldy as the networks can be large and the variables can have multiple states, often leading to errors and offhand quantification. Instead of using CPTs at component nodes, the fragility calculation can be performed using "simulation" or continuous nodes in AgenaRisk®. For instance, seismic fragility functions are often represented using lognormal distributions and the probability of failure of the component is obtained by applying the standard normal cumulative distribution function (CDF), as shown below:

$$F_R(x) = \Phi\left[\frac{\ln(x/m_R)}{\beta_R}\right] \qquad \text{Eq. (8)}$$

in which, $\Phi[.]$ is the standard normal probability integral, m_R is the median fragility, and $\beta_R = \sigma_{lnR}$ is the logarithmic standard deviation (or dispersion) of the fragility.

Rather than externally calculating and populating large CPTs, the following method can be used as shown in Figure 4, where the dashed borders indicate nodes that are included for arithmetic calculations that render a large CPT at the damage state node, "EDG EQ Failure", unnecessary. The probability distribution at the "Earthquake PGA" node is discretized and the extent of discretization would determine the size of the CPT at "EDG EQ Failure", if a direct dependence was defined between hazard and damage state nodes. Instead, the conditional probability distribution of simulation node "edg_eq_cont" is given by the fragility function of form $\left[\frac{\ln(x/m_R)}{\beta_R}\right]$, where x is substituted by the PGA value from its parent. The simulation node edg_normcdf calculates the standard normal cumulative distribution function for the distribution of values in its parent node, "edg_eq_cont." AgenaRisk® does not have an in-built approximation for the calculation of the standard normal operator Φ, but instead, a suitable arithmetic approximation can be used (Yerukala and Boiroju, 2015). Now, the result at node "edg_normcdf", is a continuous distribution in [0,1] or [-1,1], depending on the approximation used for Φ. The mean value of "edg_normcdf" will correspond to the failure probability of the component, with the "sign_edg" merely acting to obtain a positive value of failure probability in

the case “edg_normcdf” is in the range [-1,1]. Using what is called the “binomial trick” (Fenton, 2015), the continuous distribution can be converted to a Boolean node giving the damage state probabilities. The advantage of using this method is that fragility calculations are performed fully within the BN, and it does not require population of large CPTs in the case of a discretized hazard distribution. If the hazard distribution can be fit to a parametric distribution, this method also allows for the hazard node to remain continuous without the need for computationally costly discretisations. If required, further uncertainty may be accounted for by using an appropriate lognormal distribution in a simulation node, as parent to “edg_eq_cont”, from which the fragility parameters m_R and β_R can be sampled.

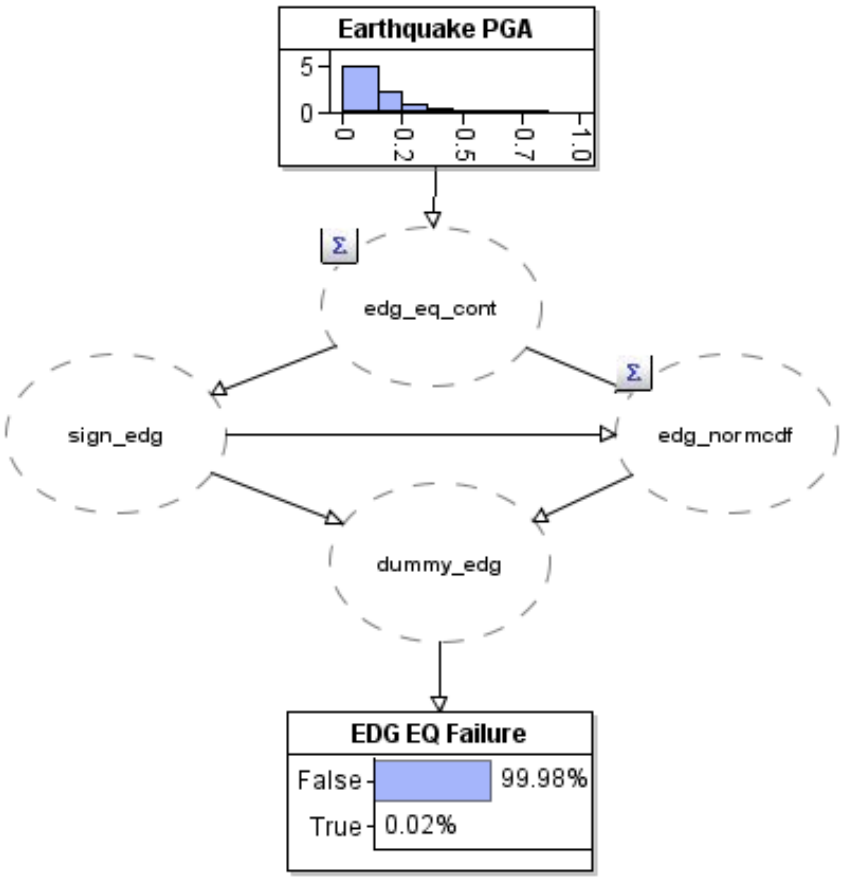

Figure 4: Calculation of damage states within BNs, using fragility functions

4 Project accident scenario and subnetworks development

The details of the project accident scenario and subnetwork development are discussed in NARSIS deliverables D3.2 (Mohan et al., 2021) and D4.5 (Kaszko et al., 2021). A summary is presented here. Figure 5 presents a flowchart of the generic methodology for developing subnetworks, for the use of BNs in NPP risk assessment. This methodology is not limited to NPPs and can also be applied in other industries, for e.g. chemical plants or aerospace applications.

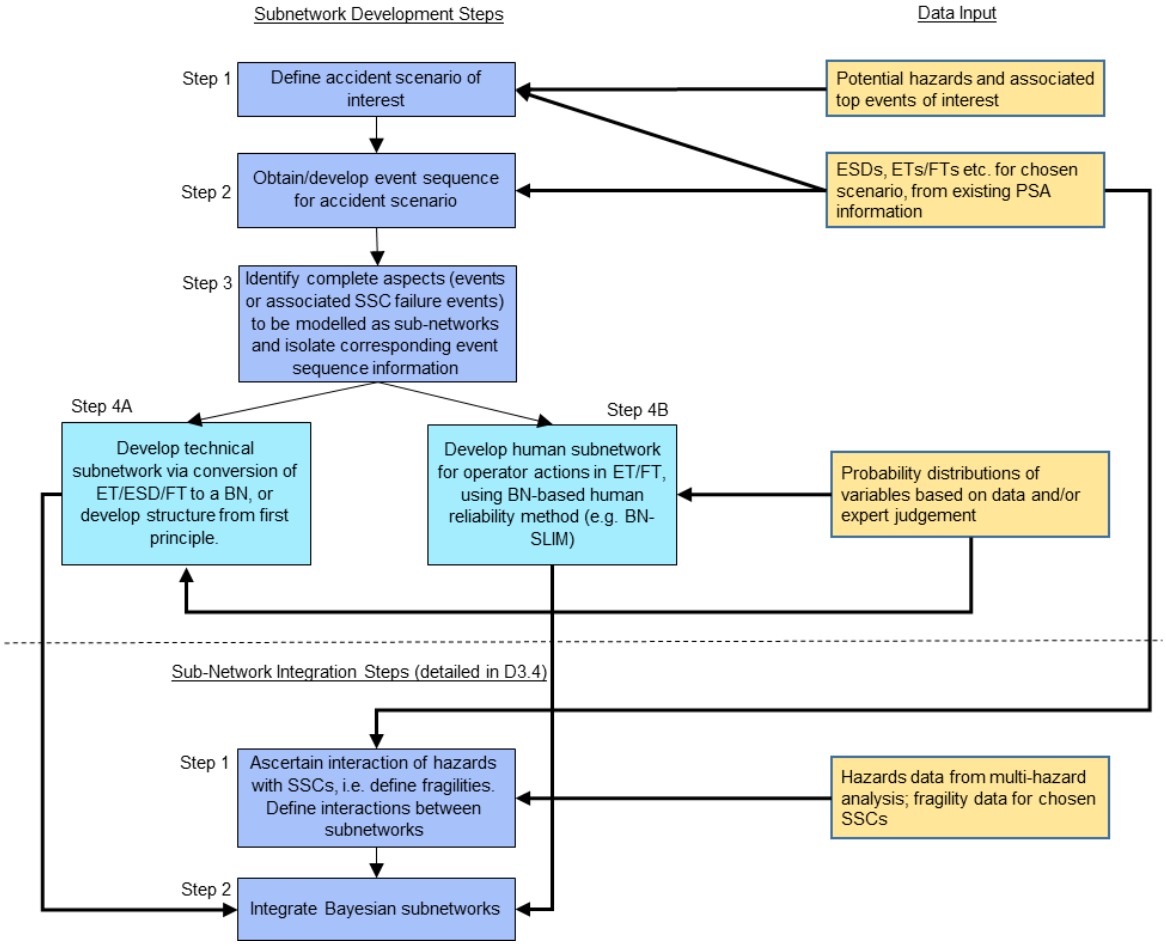

Figure 5: Generic methodology for development of Bayesian subnetworks for external hazard related NPP accident event. The subnetwork development methodology was applied to the project accident scenario defined herein (Mohan et al., 2021).

Project Accident Scenario

- Loss of offsite power (LOOP) has occurred following one or more external hazard events
- During the LOOP situation, failure of all (of four) emergency diesel generators (EDGs) would lead to a station blackout (SBO) situation
- Following SBO, failure of the steam generator (SG) used for residual heat removal (RHR) or partial cool down (PCD), would lead to failure of secondary cool down (SCD).

Hence, risk assessment of the project accident scenario aims to evaluate the probability of having SBO and SCD failure following LOOP induced by external hazard events.

The BN-based methodology is implemented to model the above project accident scenario. The design details of the various SSCs considered within this example are not of primary importance, and hence, their accuracy or completeness are not critical to this study. The

purpose of this example is to demonstrate the use of BNs in NPP risk assessments and present the advantages and disadvantages of adopting the BN framework. Nevertheless, the project accident scenario is represented with sufficient complexity.

The NPP considered in this case, is the virtual power plant (VPP) developed as part of WP4 within the NARSIS project (Bruneliere et al., 2018). The VPP is a generic generation III+ NPP, whose associated event and fault trees are obtained from deliverable D4.1 (Bruneliere et al., 2018).

Hazards

While the VPP is developed using a specific design, there is no specific location in Europe associated with the VPP. Thus, for the consideration of external hazard events, a decommissioned NPP based in Mülheim-Kärlich, Germany is chosen as the site of interest. The VPP does not correspond with the actual design details of the Mülheim-Kärlich NPP. The relevant hazards at this site are discussed as part Deliverable D1.6 (Daniell et al., 2019). For the purpose of this report, the following hazards were considered – earthquake and flooding, as in D4.5 (Kaszko et al., 2021).

Event and fault trees

As mentioned above, event trees corresponding to project accident scenario are obtained from deliverable D4.1 (Bruneliere et al., 2018). Figure 6 shows the event progression from LOOP to SBO, while Figure 7 shows the event progression from SBO to SCD (denoted as SCD_11 in the event tree). The description of function events and corresponding codes in Fig. 9 and Fig. 10 are not presented here and may be found in D4.1 (Bruneliere et al., 2018).

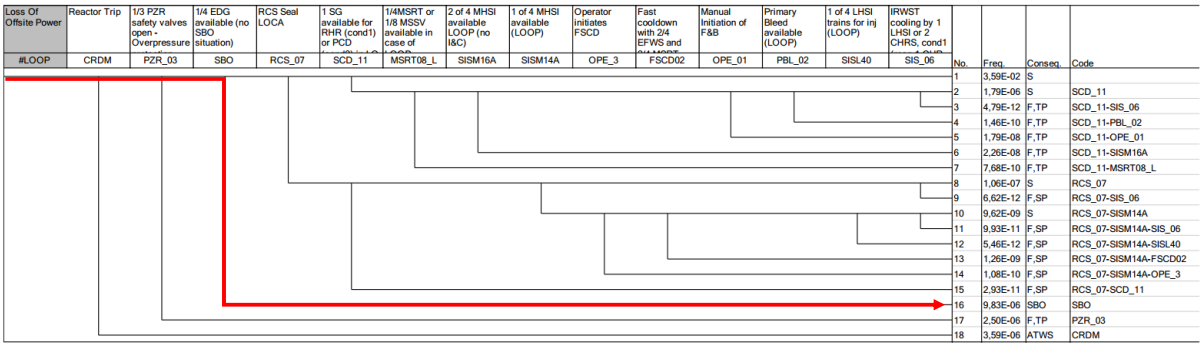

Figure 6: Event tree for progression from loss of offsite power to station blackout

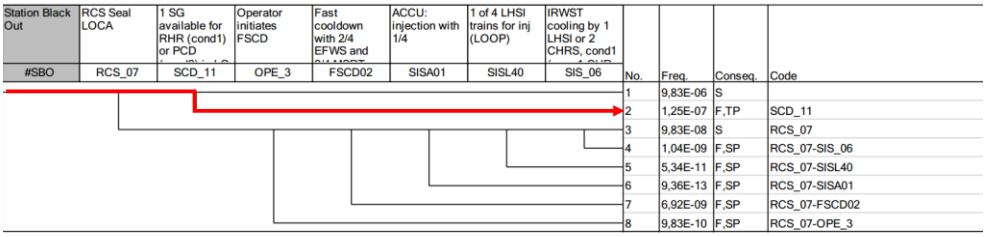

Figure 7: Event tree for progression from station blackout to secondary cool down failure

4.1 SBO subnetwork

This subnetwork pertains to the fault tree leading to SBO, during LOOP. Since existing information from a traditional PSA approach is available, it is efficient to use this to construct a BN. The subnetwork is constructed by converting the fault tree associated with the event tree shown in Figure 6. Figure 8 shows the BN corresponding to SBO fault tree, including common cause failure (CCF) events.

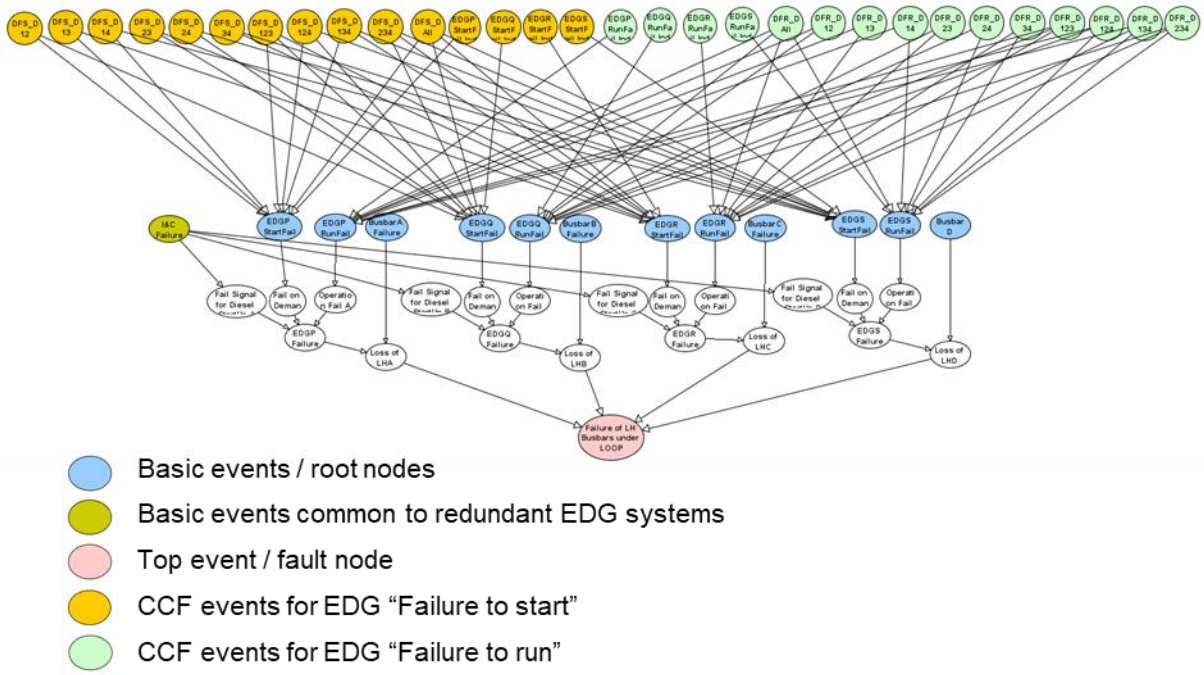

Figure 8: Station blackout Bayesian network (SBO BN)

4.2 SCD_11 subnetwork

Similar to the SBO BN, the SCD_11 subnetwork is constructed by converting the corresponding event and fault trees. Figure 9 shows the SCD_11 BN including all CCFs. This network also consists of the operator action that is modelled in the human subnetwork discussed later.

Both the SBO and SCD_11 networks demonstrate the ability of equivalent conversion of event and fault trees to BNs without loss of information or capabilities.

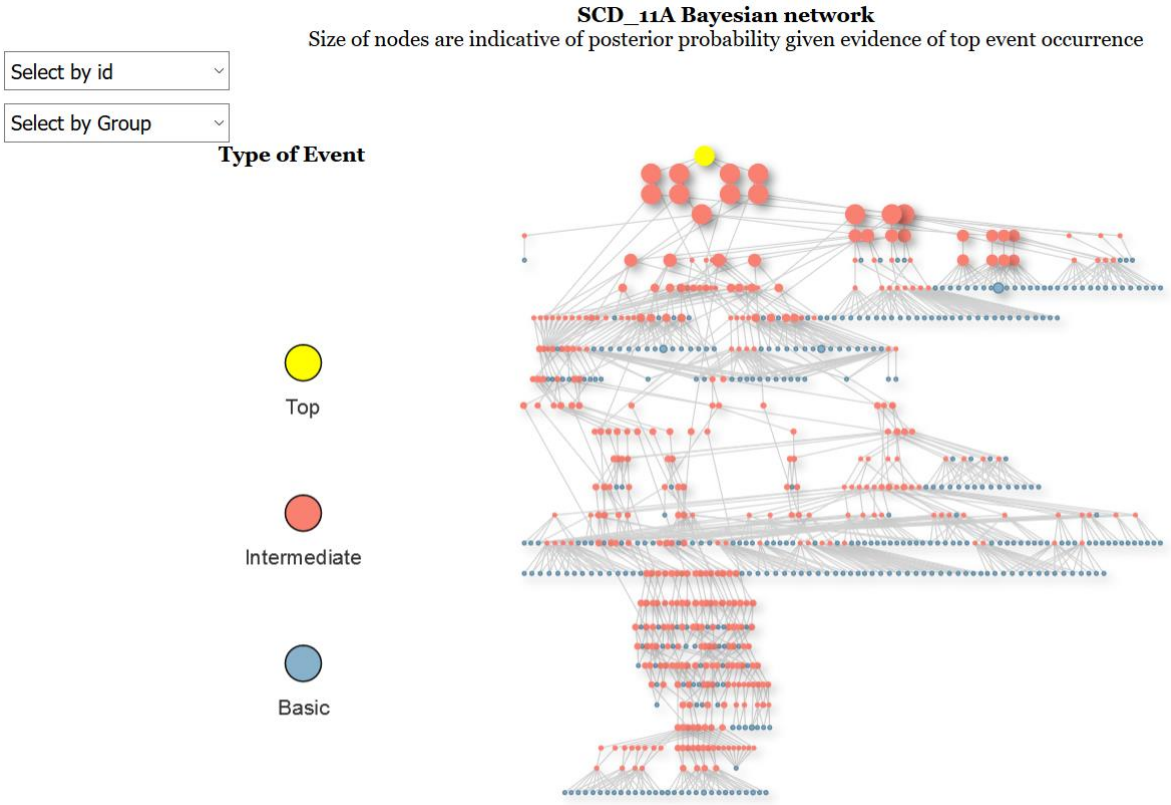

Figure 9: SCD_11 BN

4.3 Flood defence subnetwork

The development of the flood defence subnetwork and its results are presented in Mohan et al. (2019) and D3.2 (Mohan et al., 2021). This subnetwork (shown in Figure 10) acts as a surrogate model to an advanced numerical model – following the random finite element method (Fenton and Griffiths, 2008; Hicks and Samy, 2004) - used to estimate reliability of the flood defence dike.

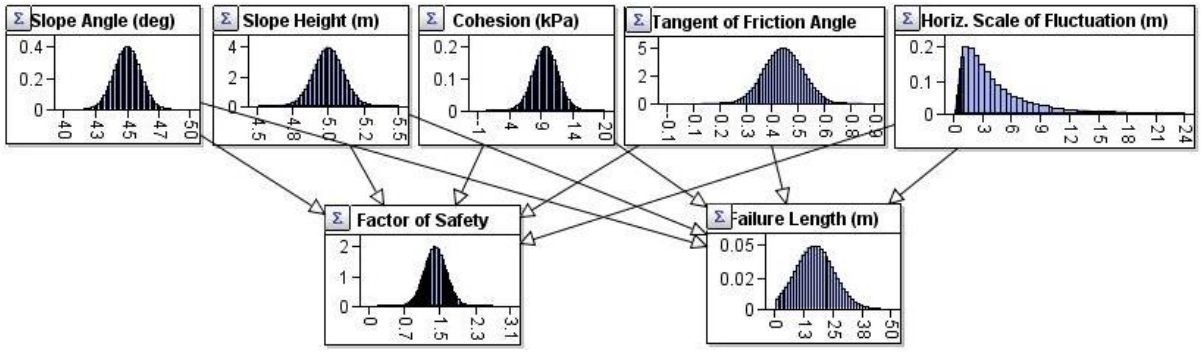

Figure 10: Flood defence BN

The concepts demonstrated using the flood defence BN may be used in building surrogate models for any system (Mohan et al., 2019). The BN was shown to be a convenient tool for reliability updating while providing a visual representation of the interaction of model parameters, both amidst themselves as well as with the final reliability estimate. The value of additional testing on the system was also evaluated from the BN. This subnetwork also demonstrates the capability of BNs to handle continuous probability distributions.

4.4 Subnetwork modelling hazard-fragility interaction

The next subnetwork models the interaction between hazards and fragilities using the example of seismic risk to an EDG building at an NPP. Vector-valued fragility functions were developed as part of this effort to quantify the interaction between multiple intensity measures (IMs) – spectral acceleration at different time periods – and the SSCs (concrete structure and EDGs). The hazards, components and their vector-valued fragility interactions were modelled using BNs (Gehl and Rohmer, 2018). Figure 11 shows the structure of the BN used to model probability of occurrence.

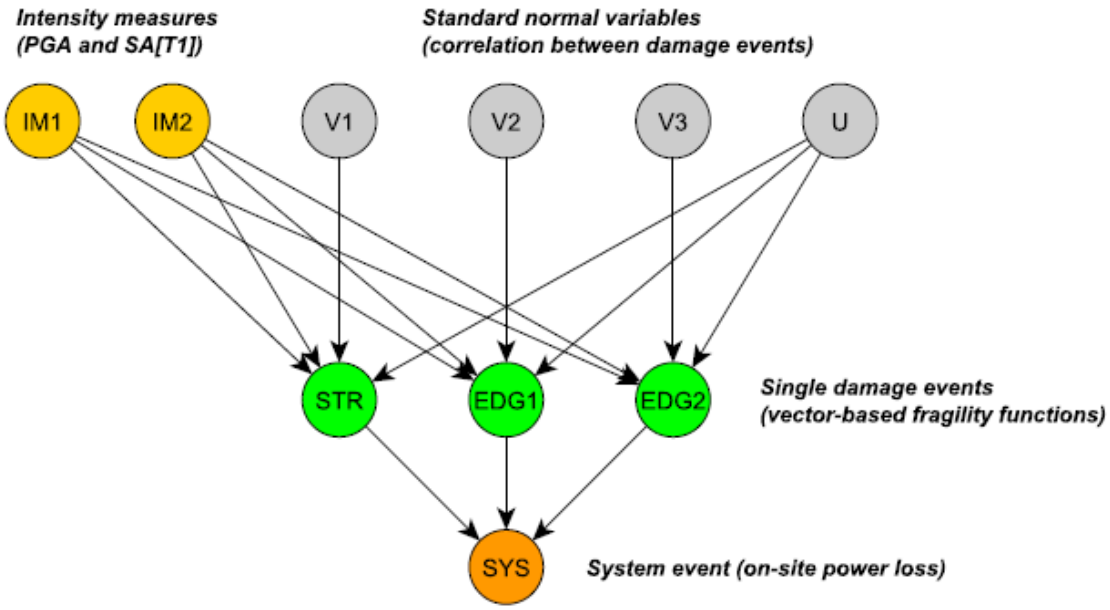

Figure 11: BN modelling hazard-fragility interaction

4.5 Human subnetwork

The last subnetwork is a BN estimating the human error probability (HEP) associated with an operator action in the SCD_11 BN – operator fails to start and control the emergency feedwater system (EFWS). The BN-SLIM procedure developed as part of the NARSIS project is used for HEP estimation (Abrishami et al., 2020). Such a BN-based method allows for direct integration of the HEP estimation model with the overall risk assessment BN for the accident scenario. In addition, structured expert judgement elicitation was used in populating the probability distributions of performance shaping factors (PSFs) for the operator action. This demonstrates the ability of BNs to easily integrate expert opinion while representing and tracking the associated uncertainty. The details of the human reliability BN, including the description of PSF ratings (R1 to R9) and the expert elicitation process, are presented in Abrishami et al. (2020) and D3.2 (Mohan et al., 2021). Figure 12 shows the human reliability BN.

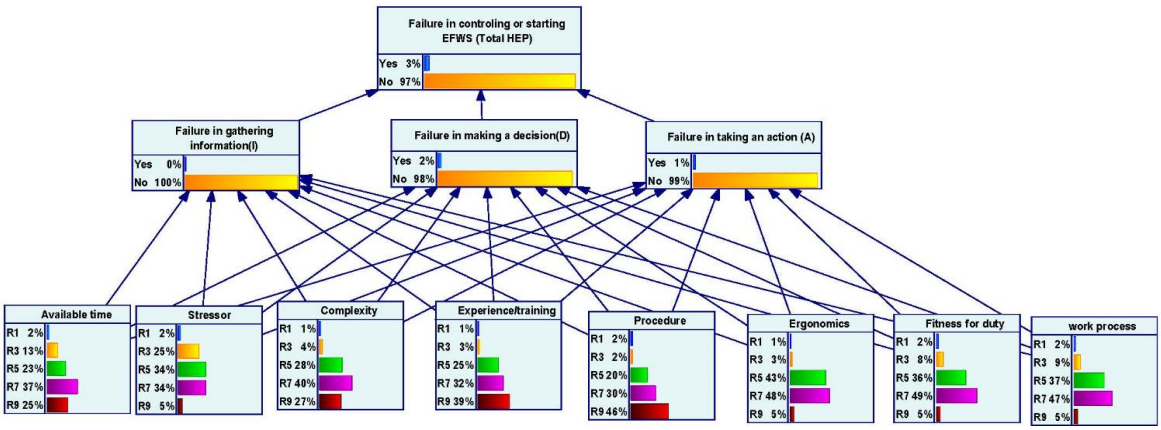

Figure 12: Human reliability BN

5 BN-based integration for project accident scenario

In this section, the subnetworks listed previously are integrated along with their interaction with external hazards, within the project accident scenario, to demonstrate the BN-based method for a realistic case. Specifically, the SBO, the SCD_11, the flood defence BN and the human reliability BN are integrated along with their interactions with external hazards – earthquake and flooding events.

5.1 Existing PSA approach

For the given accident scenario event and fault trees were constructed and the accident probability was evaluated using both a conventional PSA approach as well as a BN-based approach in deliverable D4.5 (Kaszko et al., 2021). The SBO case was used to compare the methods, and a summary is presented here. The basic approach and assumptions for the external hazard integration are listed here:

- Earthquake and flooding were chosen as the external hazard events of interest.
- Basic event and fault trees for the SBO and SCD_11 were used to develop seismic and flooding hazard trees. The basic fault trees would correspond to a random failure event, while the hazard trees would represent the failure probability induced by hazard events.
- If the equipment is flooded, it is assumed to have failed completely. This also implies that flooded equipment cannot be damaged by earthquakes and hence, these components and associated CCF events would not feature in the seismic tree.

The total failure probability of failure including multiple hazards can be obtained from a general formula:

$$P = P(Failure|NoExternalHazard)P(NoExternalHazard) + P(Failure|ExternalHazard)P(ExternalHazard) \quad \text{Eq. (9)}$$

The comparison of the two methods and their advantages and disadvantages were presented in D4.5.

When all the models are created and appropriate modifications are made, this formula can be specified for the considered case, as (Kaszko et al., 2021):

$$P = P_{basic}P_{NH} + \sum_{i=1}^{n}\left(P_{Fl,EQ} + P_{EQ,Fl}\right) + \sum_{i=1}^{m} P_H \quad \text{Eq. (10)}$$

Where, n is the number of flooding intervals, m is the number of other hazards P_{basic} is the probability of failure of a basic model, P_{NH} is the probability of no external hazards, $P_{Fl,EQ}$ is the probability of failure only due to flooding (in case of the occurrence of flooding and earthquake), $P_{EQ,Fl}$ is the probability of failure only due to earthquake (in case of the occurrence of earthquake and flooding), and P_H is the probability of failure due to other possible hazards (including single flooding or earthquake). This means that the first term describes probability of the failure in case of no occurrence of external hazards. The second term assumes occurrence of flooding and earthquake as multiple-hazards. The third term includes other possible hazards such as single hazards (e.g. Flooding, Earthquake etc.) and can include other multiple-hazards.

Further details of the developed PSA model, the results and comparison with BNs is presented in D4.5 (Kaszko et al., 2021).

5.2 BN-based approach

The integration of external hazards with the SBO BN, based on the above assumptions, is first presented to demonstrate the BN approach and understand some differences with the existing PSA approach. Later other subnetworks are included to present the overall case, as these subnetworks (the flood defence BN and human reliability BN) were not represented in the existing PSA model in deliverable D4.5. Accordingly, the hazard data used in this demonstration of multi-hazard integration with the SBO BN is exactly same as what was used in D4.5 in the existing PSA approach (Kaszko et al., 2021). The actual flooding and earthquake data from Mülheim-Kärlich, Germany presented in D1.6 (Daniell et al., 2019) is used in the next section where all the subnetworks of interest are integrated.

The existing PSA model employs separate hazard trees for the different hazards – earthquake and flooding. Within flooding, separate trees are used for each intensity (no flooding, flooding between 0.01-4m and 4+m) based on the different assumptions associated with each of them. Within the seismic tree, three different hazard curves are used depending on the multi-hazard interaction between different the three flooding levels and earthquake PGA (Figure 13). The frequency of the PGA at 0.9-1.0+g is high due to the inclusion of higher PGAs in this bin. The hazard data in this section is only for demonstration, chosen to exactly match the data used in D4.5 (Kaszko et al., 2021). This logical structure from the existing PSA approach is modelled in two different ways using BNs to highlight the characteristics, possibilities and limitations of the BN method.

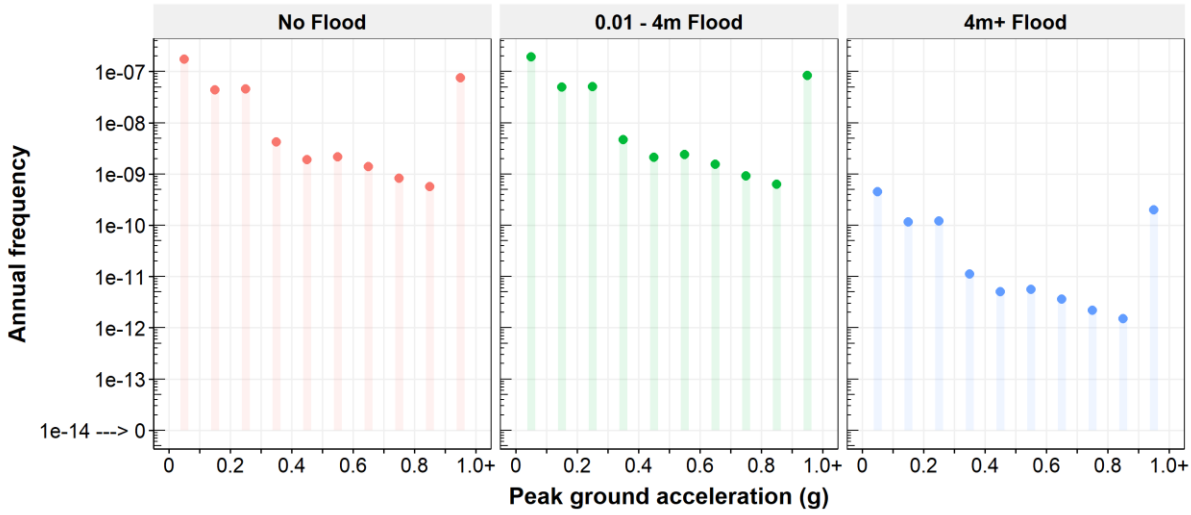

Figure 13: Multi-hazard histograms used in discretized conditional probability distributions of PGA given flooding level (or in subnetworks corresponding to different flooding levels)

5.2.1 Object-Oriented Bayesian network approach

Firstly, a similar logical structure is reproduced using BNs, wherein different subnetworks are used to model each corresponding hazard tree in the existing PSA model. The logic of the event trees is then integrated in the main BN model (Figure 14), featuring the interactions between subnetworks. This demonstrates both the possibility of equivalent implementation in BNs as well as the use of object oriented BNs (or OOBNs) via subnetworks.

The workings of OOBNs and their features can vary significantly depending on the software programs used and the inference algorithms implemented within them. In this study, we use AgenaRisk® to demonstrate the use of subnetworks (or 'risk objects' as termed by the program), which allow the separation of various hazard cases, similar to the existing PSA approach using event and fault trees. The interaction between risk objects is defined in the main model and is made possible by the use of "input nodes" and "output nodes" within the risk objects. Input nodes receive the marginal distribution calculated from the corresponding

output nodes in ancestral risk objects. A key point to note when using risk objects in AgenaRisk® is that both predictive and diagnostic inference is possible within risk objects, whereas only predictive inference can be performed between risk objects. In other words, between risk objects, marginal distributions from one ancestral risk object are sequentially passed to a connected, descendant risk object.

In Figure 14, each white box indicates a separate subnetwork (corresponding to a separate fault tree or event tree sequence in the existing PSA approach). The blue and green boxes are input and output nodes respectively. It can be seen how the output node from each subnetwork connects to an input node in another subnetwork. The final subnetwork "F. Sum All" provides the overall multi-hazard probability, *P*, as in Eq. (10). This main BN model involving subnetworks produces the exact same probabilities as the existing PSA approach, while providing the advantages of using BNs (for e.g. Bayesian updating, diagnostic inference, see D3.2 (Mohan et al., 2021)). However, as mentioned earlier, a limitation of using OOBNs in AgenaRisk® is that diagnostic inference is not possible between subnetworks (or risk objects).

Using this main BN model, the probabilities of SBO for different flooding cases are calculated and presented in Table 1. The results are identical to the point estimate probabilities obtained from the existed PSA model in D4.5 (Kaszko et al., 2021), confirming the equivalence of the BN with the existing PSA approach. The results from the earthquake trees (or subnetworks) may differ but are not linked to any methodological factors associated with fault trees or BNs and hence, are not important to the scope of this study. The differences are merely due to the fragility models used in the existing PSA approach and associated uncertainty analyses, which if required, may be reproduced within BNs.

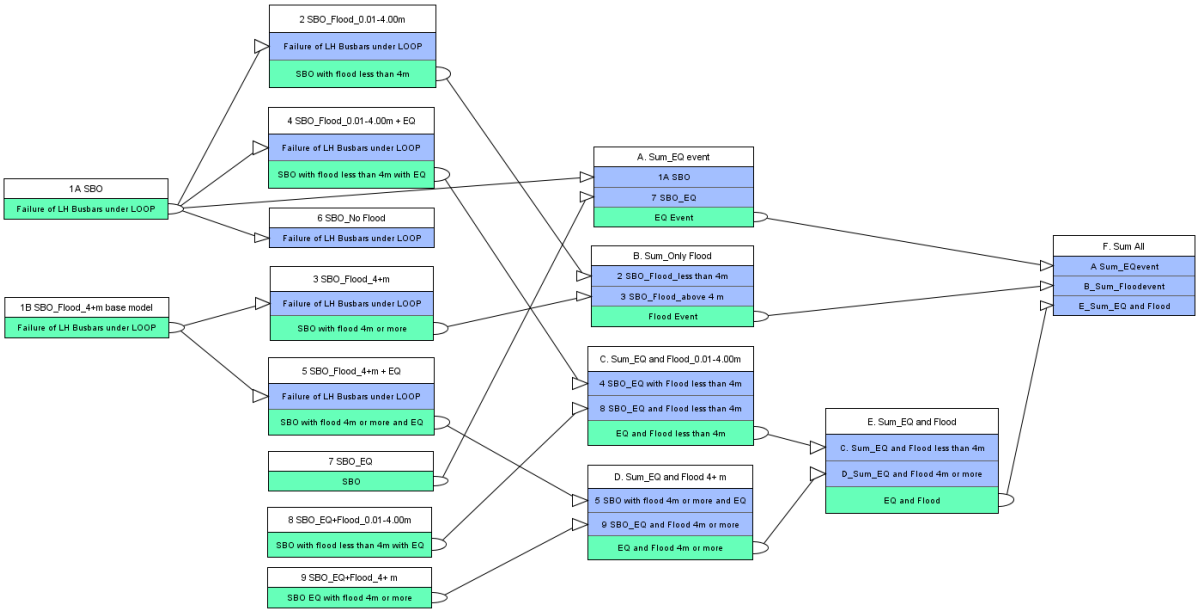

Figure 14: Main BN model, involving various subnetworks corresponding to hazard trees in the existing PSA approach

Table 1: SBO failure probabilities for different floodings

	Name	**Point Est. Prob.**
1	SBO failure – Flooding+Earthquake 0.01-4m	2.40E-05
2	SBO failure – Flooding+Earthquake 4+m	2.15E-06
3	SBO failure – Flooding 0.01-4m	2.69E-05
4	SBO failure – Flooding 4+m	2.34E-06
5	SBO failure – No flooding	2.21E-04

5.2.2 Unified BN approach

Alternately, the logical structure achieved using several fault trees and event trees can be modelled within a unified BN (see Figure 15) to fully take advantage of diagnostic capabilities across various hazard scenarios. It can be seen that with the addition of only 2 hazard nodes and 3 component failure nodes, the SBO BN in Figure 8 is transformed to include all multi-hazard scenarios previously modelled in several hazard trees (or subnetworks). In fact, the 3 failure nodes can also be integrated into existing component (random) failure nodes in the SBO BN, but separating hazard damage from other random failures can be useful for diagnostics. It is possible to include all hazard scenarios in a single, unified BN because the logical interactions can be included within conditional probability tables (CPTs) of the nodes of the BN, rather than using several subnetworks. For example, Figure 16 shows the CPTs at "Flood" and the "Earthquake PGA" node. The different levels of flooding, for which individual BNs were used as subnetworks (or individual fault trees in the existing PSA approach), are now included as multiple states of the "Flood" node, with associated probabilities of occurrence. Hence, dependencies between hazard nodes and their interaction with components (fragilities) can be modelled within the conditional probability relationships at the nodes. This represents a more direct modelling of dependence between variables and ensures all dependencies are considered without missing any interactions while transitioning between fault trees and event trees. The possibility of using multi-state variables in BNs allows the reduction of several fault and event trees to a single BN. Since all hazard scenarios are considered within a single BN, the top event directly yields the overall probability of SBO – probability, *P* in Eq. (10). Within the unified BN in Figure 15, the dashed edges between the "Earthquake PGA" node and the component damage nodes indicate that there are some hidden nodes. These nodes are hidden since they are not events of interest for the scenario, but merely nodes to carry out arithmetic calculations for component fragility, given earthquake PGA (based on Section 3.3.2). Alternatively, the fragility functions can be applied outside the BN and input into the damage state nodes as CPTs. The computational differences between these two types of fragility calculations is discussed later in Section 5.5.

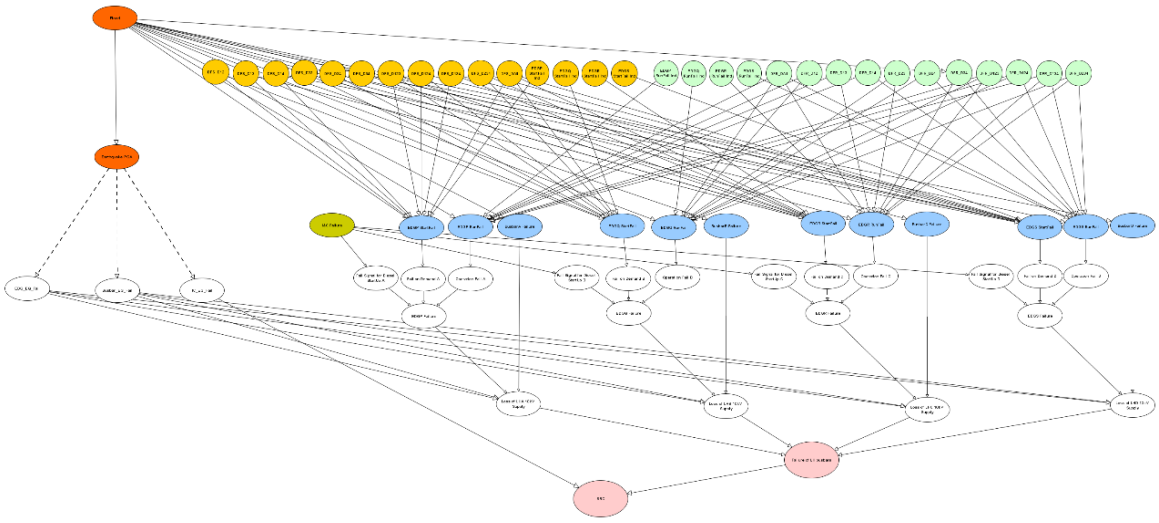

Figure 15: Unified BN model including all multi-hazard scenarios

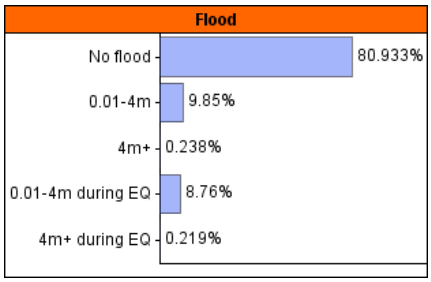

(a)

	Flood Level				
Earthquake PGA	**No flood**	**0.01-4m**	**4m+**	**0.01-4m during earthquake**	**4m+during earthquake**
0.0 - 1.0E-20	9.999996400E-01	9.999996400E-01	1.000000000E+00	9.999996400E-01	1.000000000E+00
1.0E-20 - 0.1	1.72E-07	1.91E-07	4.52E-10	1.91E-07	4.52E-10
0.1 - 0.2	4.41E-08	4.90E-08	1.16E-10	4.90E-08	1.16E-10
0.2 - 0.3	4.57E-08	5.07E-08	1.20E-10	5.07E-08	1.20E-10
0.3 - 0.4	4.21E-09	4.67E-09	1.11E-11	4.67E-09	1.11E-11
0.4 - 0.5	1.90E-09	2.11E-09	4.99E-12	2.11E-09	4.99E-12
0.5 - 0.6	2.14E-09	2.37E-09	5.62E-12	2.37E-09	5.62E-12
0.6 - 0.7	1.38E-09	1.53E-09	3.63E-12	1.53E-09	3.63E-12
0.7 - 0.8	8.26E-10	9.17E-10	2.17E-12	9.17E-10	2.17E-12
0.8 - 0.9	5.67E-10	6.30E-10	1.49E-12	6.30E-10	1.49E-12
0.9 - 1.0	7.55E-08	8.38E-08	1.99E-10	8.38E-08	1.99E-10

(b)

Figure 16: Conditional probability distributions at (a) "Flood" node and (b) "Earthquake PGA" node in the unified BN

The multi-hazard impact on the probability of the SBO can be calculated via forward (or predictive) inference in the BN. Figure 17 shows the probability of SBO occurrence during flooding and earthquake events, for different values PGA. Next, various PGA values are applied as evidence to the BN, and using Bayesian updating, corresponding probabilities of SBO occurrence are obtained from the network. Figure 18 shows the variation of SBO probability conditional on various PGA values. The values in Table 1 can be reproduced, as well, with the unified BN by setting evidence of no earthquake (PGA = 0) and required flooding level, demonstrating the equivalence with the OOBN and existing PSA methods.

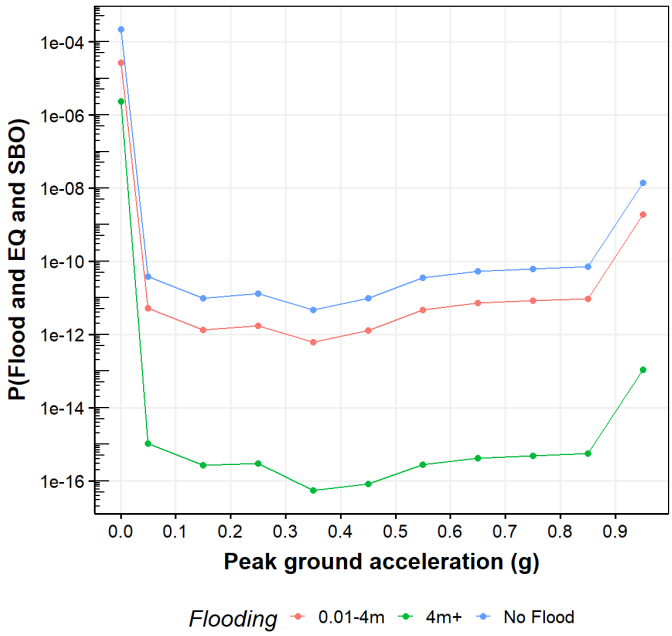

Figure 17: Probability of SBO during combined flooding and earthquake events, calculated using the unified BN

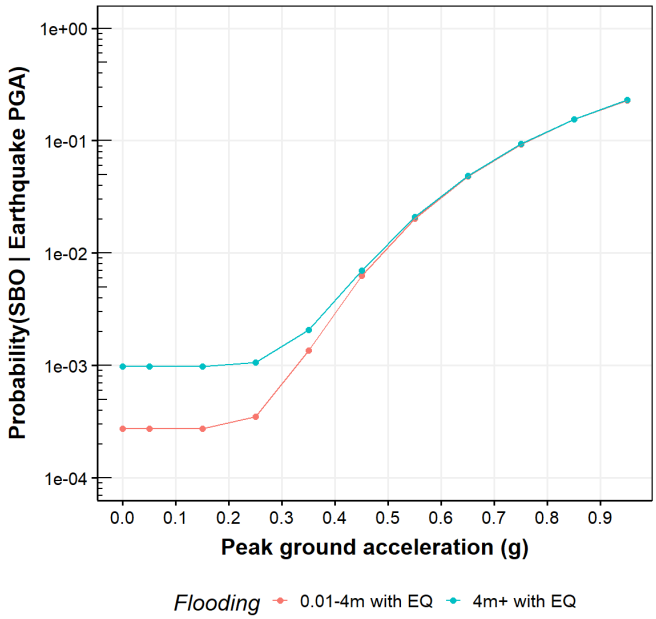

Figure 18: Conditional probability of SBO given Earthquake PGA, calculated using the unified BN

As part of sensitivity and importance analysis, the posterior probability of all nodes in the BN is calculated by setting evidence of top event occurrence (SBO = “True”). Posterior probabilities can be used both for diagnosis but as well for importance measures. Figure 19 shows the impact of various node states on the probability of top event occurrence, as a measure of sensitivity. Figure 19a shows the tornado plot for CCF events, showing their impact on SBO occurrence. Figure 19b presents the same for basic events and the hazard nodes. For instance, the P(SBO = ”True”) varies from less than 10E-03 when P(DFR_All = “False”), to 0.995 when P(DFR_All = “True”) while no evidence is provided to any other node in the BN, where DFR_All represents the CCF event involving the “failure to run”, of all four EDGs. For continuous (or discretised) nodes such as earthquake PGA, the upper and lower percentile indicate the probability of SBO at 25th and 75th percentile values of PGA.

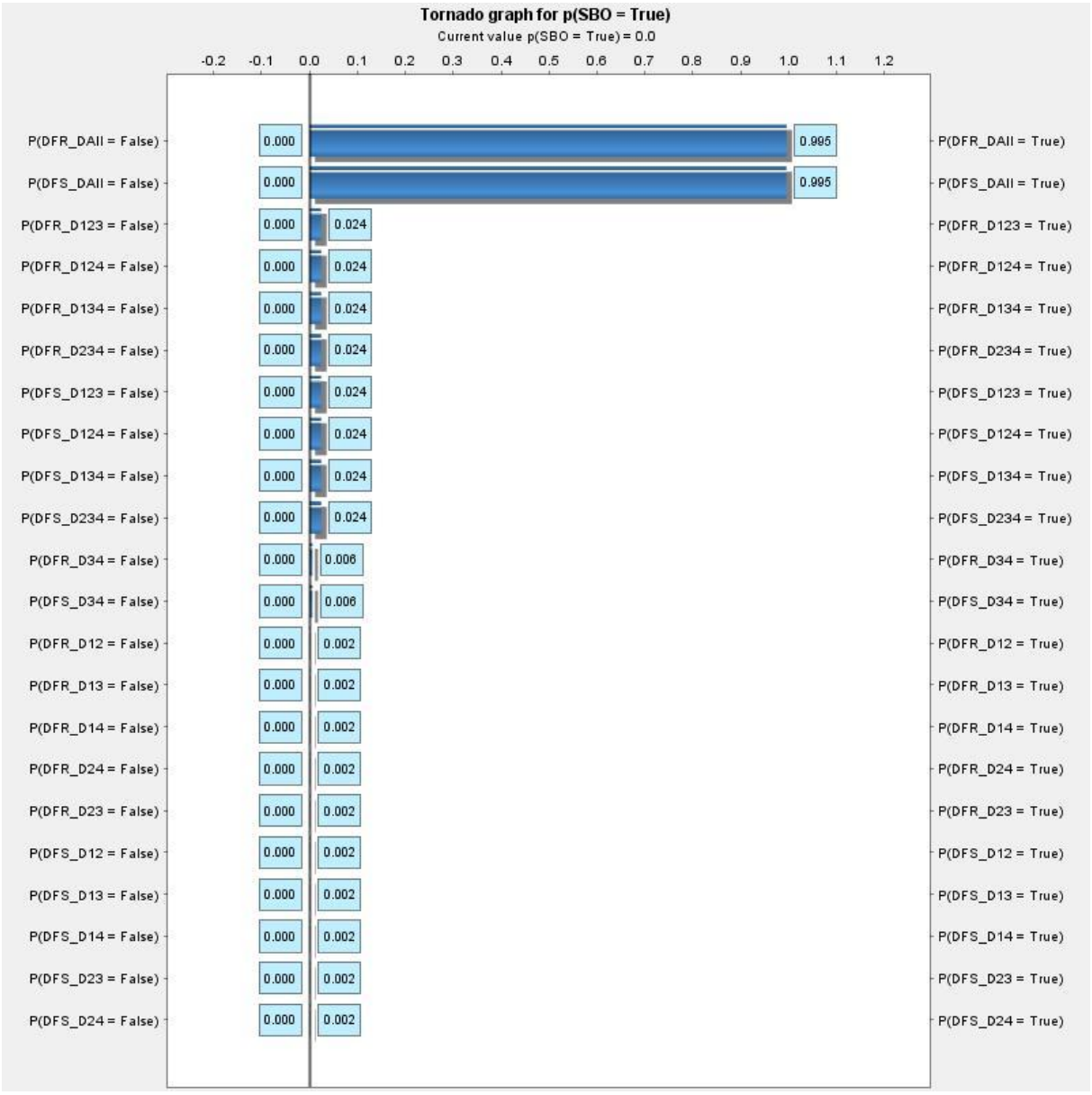
Tornado graph for p(SBO = True)
Current value p(SBO = True) = 0.0
-0.2 -0.1 0.0 0.1 0.2 0.3 0.4 0.5 0.6 0.7 0.8 0.9 1.0 1.1 1.2
P(DFR_DAll = False) 0.000 0.995 P(DFR_DAll = True)
P(DFS_DAll = False) 0.000 0.995 P(DFS_DAll = True)
P(DFR_D123 = False) 0.000 0.024 P(DFR_D123 = True)
P(DFR_D124 = False) 0.000 0.024 P(DFR_D124 = True)
P(DFR_D134 = False) 0.000 0.024 P(DFR_D134 = True)
P(DFR_D234 = False) 0.000 0.024 P(DFR_D234 = True)
P(DFS_D123 = False) 0.000 0.024 P(DFS_D123 = True)
P(DFS_D124 = False) 0.000 0.024 P(DFS_D124 = True)
P(DFS_D134 = False) 0.000 0.024 P(DFS_D134 = True)
P(DFS_D234 = False) 0.000 0.024 P(DFS_D234 = True)
P(DFR_D34 = False) 0.000 0.006 P(DFR_D34 = True)
P(DFS_D34 = False) 0.000 0.006 P(DFS_D34 = True)
P(DFR_D12 = False) 0.000 0.002 P(DFR_D12 = True)
P(DFR_D13 = False) 0.000 0.002 P(DFR_D13 = True)
P(DFR_D14 = False) 0.000 0.002 P(DFR_D14 = True)
P(DFR_D24 = False) 0.000 0.002 P(DFR_D24 = True)
P(DFR_D23 = False) 0.000 0.002 P(DFR_D23 = True)
P(DFS_D12 = False) 0.000 0.002 P(DFS_D12 = True)
P(DFS_D13 = False) 0.000 0.002 P(DFS_D13 = True)
P(DFS_D14 = False) 0.000 0.002 P(DFS_D14 = True)
P(DFS_D23 = False) 0.000 0.002 P(DFS_D23 = True)
P(DFS_D24 = False) 0.000 0.002 P(DFS_D24 = True)

(a)

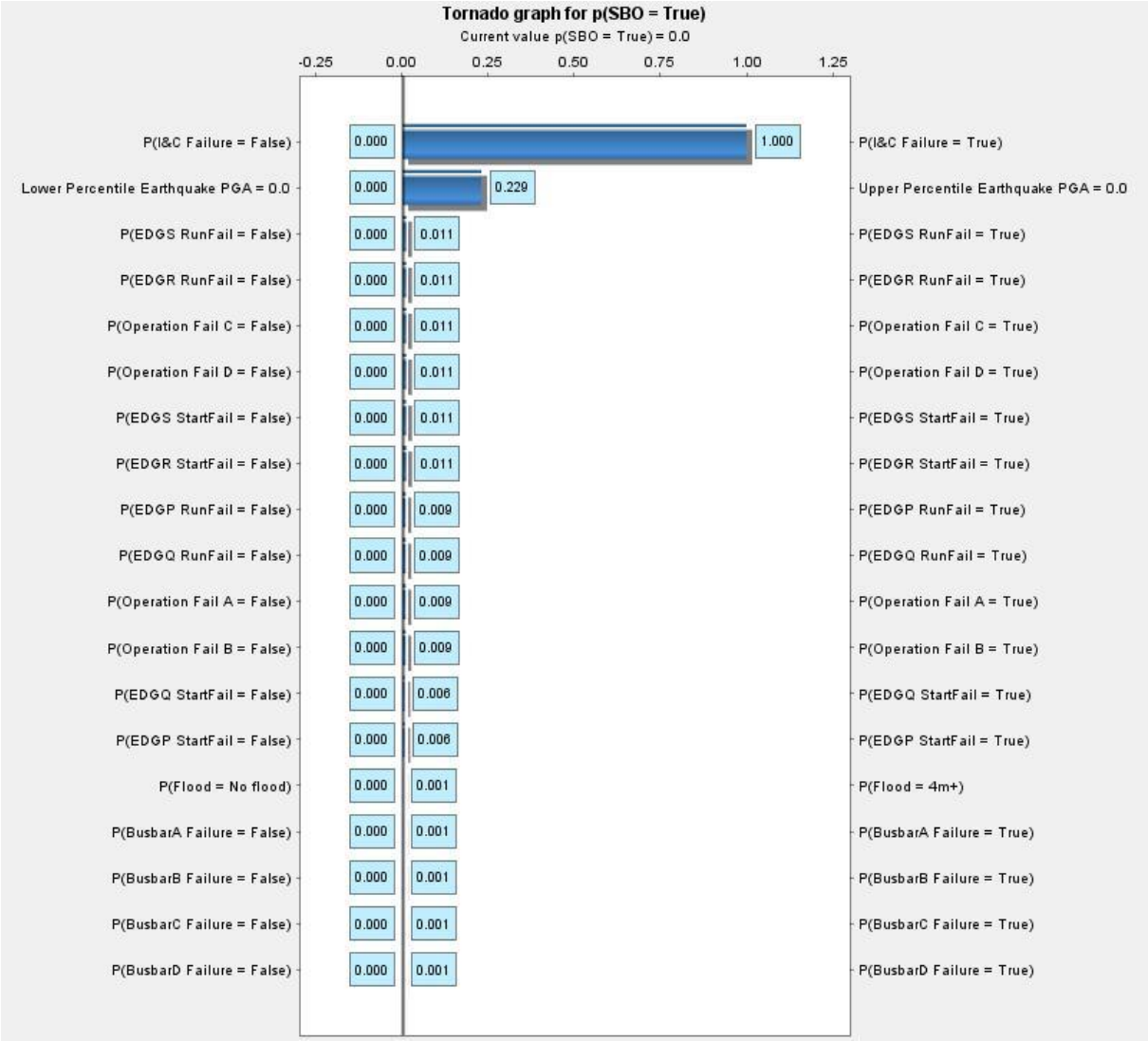

(b)

Figure 19: (a) Sensitivity of SBO event to the different states of CCF event nodes; (b) Sensitivity of SBO event to states of basic event and hazard nodes

The various advantages and disadvantages of BNs compared to existing PSA approach using event and fault trees were summarised in deliverable D4.5 (Kaszko et al., 2021). Those pertaining to multi-risk integration, specifically based on the above demonstration using the SBO BN, are summarised in Section 5.6.

5.3 Integration of subnetworks

In the previous section, the SBO BN was used to demonstrate the basic principles of multi-risk integration using BNs and the two main possibilities – a unified BN or OOBNs. Now other subnetworks - SCD_11, the flood defence BN and the human reliability BN are integrated with the SBO BN. The integration is performed using features of both the unified BN approach as well as the OOBN approach in the interest of demonstration of their combined applicability. The subnetwork pertaining to hazard-fragility interaction is not explicitly integrated here due to the absence of multiple intensity measures or vector-valued fragilities in this example accident scenario. Nevertheless, the principles of multi-hazard integration were already demonstrated in that subnetwork as it inherently included hazard impact and dependence between intensity measures (Gehl and Rohmer, 2018; Mohan et al., 2021).

During integration of the chosen subnetworks, hazard impact is assumed to be limited to the following:

(i) The flood defence dike
(ii) All applicable components in the SBO BN – EDGs (including CCF events), busbars and the instrumentation & control (I&C) system
(iii) Relevant PSFs in the human reliability BN – "Available Time" and "Stressors"; the HEP of operator action calculated from the human reliability BN feeds into the SCD_11 network

The hazard impact on several components in the SCD_11 network is not considered as it adds little value to the demonstration of the risk integration procedure, but merely adds further computational load to the BN calculations. These computational challenges associated with BNs are, of course, a limitation to BN use in PSA, which is discussed later in Section 5.5.

Below, the hazards information used and their interaction with each subnetwork is described separately. Eventually, their integration, using the unified BN approach, is presented. Although the risk integration methodology presented earlier in Section 3.2 is followed in principle, some of the steps and iterations have been internalised within subnetwork development described earlier and the hazard integration described below. Hence, the methodology is not explicitly applied in a sequential manner here, but the corresponding steps and iterations are indicated where they are implicitly implemented.

5.3.1 Hazard data

Initially, earthquake, flooding and volcano hazards were considered based on the decommissioned site at Mülheim-Kärlich, Germany, as described in deliverable D1.6 (Daniell et al., 2019) – corresponding to *Step 1* in the BN-based risk integration methodology of Section 3.2. However, on examination of the hazard probabilities, their dependence, and the SSCs involved in the project accident scenario, only earthquake and flooding events were considered as relevant hazards (as in deliverable D4.5 in the existing PSA approach). Such elimination of hazards can, in reality, also be decided in *Step 5* of the risk integration method, where the inconsequential hazard(s) would be ignored in the subsequent iteration(s) of the BN.

It is assumed that earthquake is followed by flooding, where the ground motion occurs within a period of 0-7 days when the flood water level lasts, after which the hazards are assumed to become independent (no concurrence), as the flood water level recedes.

Flooding

The flooding data shown in Table 2 is obtained based on deliverable D1.6 (Daniell et al., 2019).

Table 2: Flooding hazard - probability distribution

Flooding Height (m)	Annual Probability of Occurrence
0.0 - 0.01 (~ no flood)	8.99E-01
0.01 - 0.5	6.26E-02
0.5 - 1.0	1.22E-02
1.0 - 2.0	1.56E-02
2.0 - 3.0	4.81E-03
3.0 - 4.0	3.36E-03
4.0 - 5.0	1.88E-03
> 5.0	5.00E-04

Earthquake

The earthquake data used herein is obtained from deliverable D1.6 (Daniell et al., 2019). Both the independent hazard curve as well as the earthquake dependence with flooding are presented. At the "earthquake PGA" node of the integrated BN, the hazard curve is discretised evenly at a bin width of 0.05g, except 0.00-0.15g as this range is considered to be inconsequential based on the fragility of components. Such filtering of the hazard data can also be performed using the BN, which would comprise *Step 5* of the risk integration framework, which would then be followed by a further iteration of the BN with a more efficient discretisation of the hazard curve. The effect of discretisation on hazard data is a key aspect in the use of BNs that is, however, not investigated in this study.

Figure 20 presents the multi-hazard data for flood and earthquake events used in the unified BN.

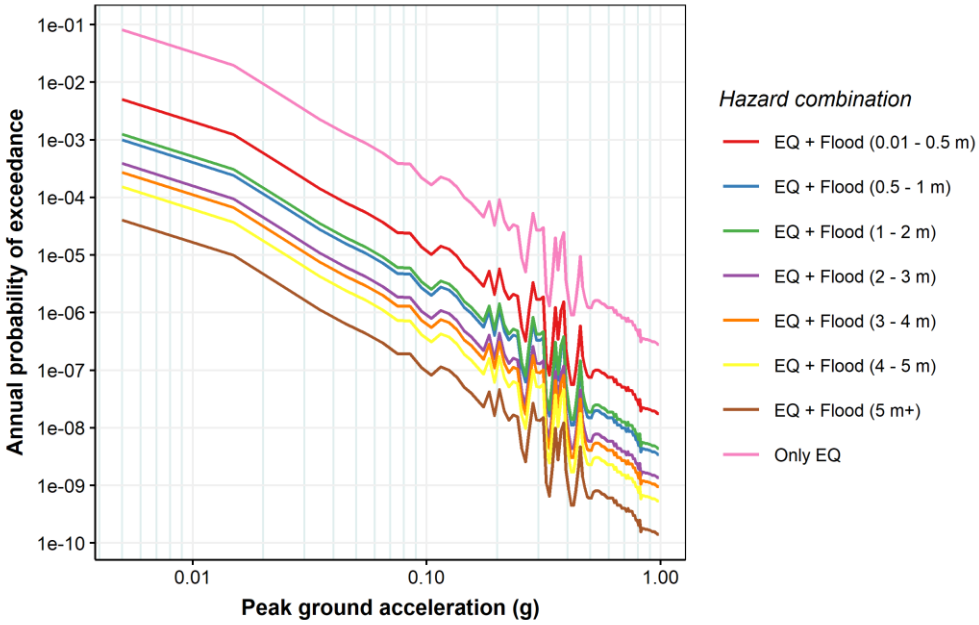

Figure 20: Combined hazard curves for earthquake and flooding events

5.3.2 Hazard impact on flood defence BN

As in the flood defence BN, the dike is assumed to be 5 m in height, higher than the lowest EDG at 4 m from the datum. The topography of the site is assumed to be flat between the dike and the EDG building. Failure of the flood defence dike can be attributed to two main causes: random failure and hazard induced failure. Of course, the flood defence fails if either case were to occur and can lead to internal flooding. The flood defence subnetwork yields the random failure probability via the distribution of factor of safety, where a factor of safety of less than 1.20 is assumed to cause dike failure based on a 95% reliability estimate. The hazard induced failure is assumed to possibly occur via three modes – overtopping due to flooding, piping failure due to flooding and global stability failure due to the joint impact of flooding and earthquake. The fragility functions used for the piping and global stability failure modes are given in Eq. (11) and are presented in Table 3:

$$F_R(x) = \Phi\left[\frac{\ln(IM/m_R)}{\beta_R}\right] \qquad \text{Eq. (11)}$$

where, $\Phi[.]$ is the standard normal probability integral, IM is the intensity measure for the respective hazard, m_R is the median fragility, and $\beta_R = \sigma_{lnR}$ is the logarithmic standard deviation (or dispersion) of the fragility.

Overtopping failure occurs, simply, if the flooding level is higher than 5 m (the height of the dike). Since all three fragility functions are based on a lognormal distribution, the fragility calculation and damage state nodes are modelled using the method described in Section 3.3.2. Figure 21 shows the part of the unified BN that pertains to the flood defence dike. The dashed lines indicate hidden nodes that were used merely for arithmetic calculations associated with the fragility functions.

Table 3: Single and multi-hazard fragility models for piping and global stability failure modes

Dike Failure Mode	Water Level Range (m)	IM	m_R	β_R
Piping (after Bachmann et al. (2013))	--	**Water Level**	3.48	0.22
Global Stability (after Tyagunov et al. (2018))	**WL (0-1m)**	**PGA**	0.1182	0.2786
	WL (1-2m)		0.1587	0.2778
	WL (2-3m)		0.1899	0.2783
	WL (3-4m)		0.2209	0.2797
	WL (4-5m)		0.2620	0.2775

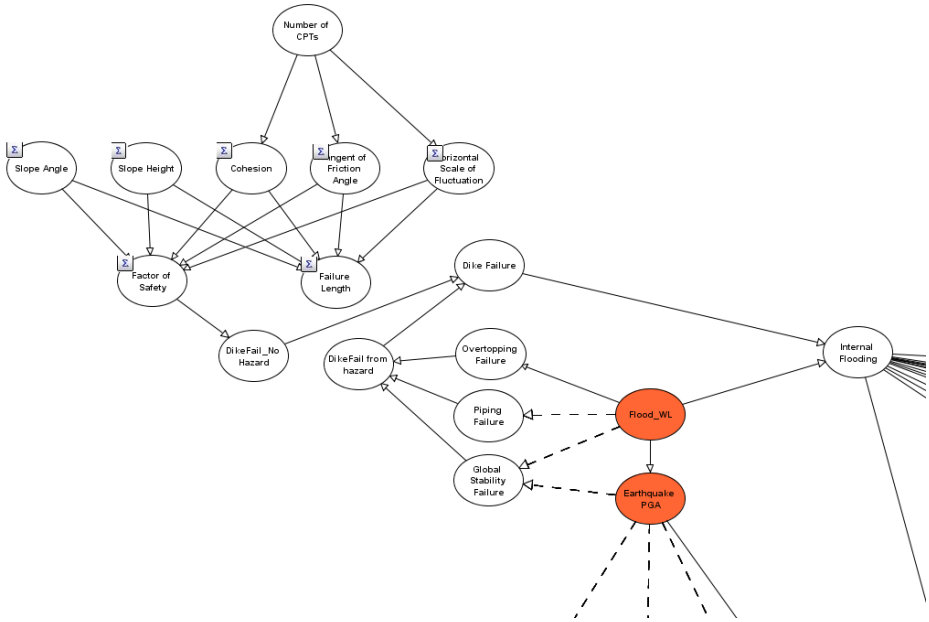

Figure 21: Hazard integration with flood defence BN

5.3.3 Hazard impact on SBO BN

Hazard impact on the SBO BN is exactly as the unified BN in Section 5.2.2, excepting two factors:

(i) A node for the internal flooding level is introduced which is dependent on the dike damage state and external flooding levels. The three states of the internal flooding node are similar to Section 5 – No flooding (0-0.01m), 0.01-4m, 4m +.
(ii) The external flood levels are divided into 8 states as in Table 2.

Figure 15 in the previous section depicts the interaction of the hazards with the SBO BN.

presents the assumed fragility parameters for the components in the SBO BN (Andersen et al., 2013). Since, all three functions are based on the lognormal distribution, the method described in Section 3.3.2 is used to model the fragility and damage states of these components.

Figure 15 in the previous section depicts the interaction of the hazards with the SBO BN.

5.3.4 Hazard impact on human reliability BN

For the purposes of demonstration, simplified assumptions are made to integrate the human reliability BN within the accident scenario. Two PSFs – "Stressor" and "Available Time" – are assumed to be impacted by the occurrence of the hazard. For the purposes of this study, it is of little value to study in detail the impact of hazards on PSFs. Instead, it is assumed that if a hazard – earthquake ground motion or internal flooding of the plant – were to occur, the PSFs would be impacted, irrespective of the intensity of the hazards. Hence, a "hazard occurrence" node is introduced which is True *when at least one of an earthquake PGA (> 0.15g) or an internal flood water level (> 0.01 m) were to occur. The CPTs of the two chosen PSFs based on occurrence or non-occurrence of hazards is shown in Table 4 Fragility parameters for components in the SBO BN (after Andersen et al. (2013))*

Component	A_m	β_r	β_u
EDG(2)	1.5	0.3	0.35
Busbar	2	0.3	0.35
I&C System	3	0.35	0.5

Table 5 and Table 6.

Table 4 Fragility parameters for components in the SBO BN (after Andersen et al. (2013))

Component	A_m	β_r	β_u
EDG(2)	1.5	0.3	0.35
Busbar	2	0.3	0.35
I&C System	3	0.35	0.5

Table 5 Conditional probability table of the PSF "Available Time" given hazard occurrence

	Hazard Occurrence	
PSF Rate	**False**	**True**
R1	0.02	0.20
R3	0.13	0.40
R5	0.23	0.30
R7	0.37	0.08
R9	0.25	0.02

Table 6 Conditional probability table of the PSF "Stressor" given hazard occurrence

	Hazard Occurrence	
PSF Rate	**False**	**True**
R1	0.02	0.20
R3	0.25	0.40
R5	0.34	0.40
R7	0.34	0.00
R9	0.05	0.00

5.3.5 Unified BN for project accident scenario

The entire SBO BN is comprised in the SCD_11 BN as the SBO event is a precursor to the failure of the secondary cool down system. Hence, the SBO BN integrated with hazards can directly be transposed into the SCD_11 BN. The flood defence BN is connected to the SBO BN via the hazards as well as the "internal flooding" node. Further, the human reliability BN is integrated with hazards via the "hazard occurrence" node and the calculated HEP is the probability of "Operator failure to start and control EFWS" node being *True* in the SCD_11

network. Hence, the human reliability BN directly fits into the SCD_11 BN. Thus, the 4 subnetworks – SBO, SCD_11, flood defence and the human reliability BN are all integrated with multiple external hazards, under one framework. The accident scenario is completed by defining a top event “LOOP_H1” which effectively checks for the joint occurrence of LOOP, SBO and SCD_11A (top event of SCD_11 BN). Figure 22 shows the unified BN with top event LOOP_H1. From Figure 22, it is evident that the visualisation of large BNs is challenging. The relationships between hazards, damage states of SSCs and end events, are no longer intelligible.

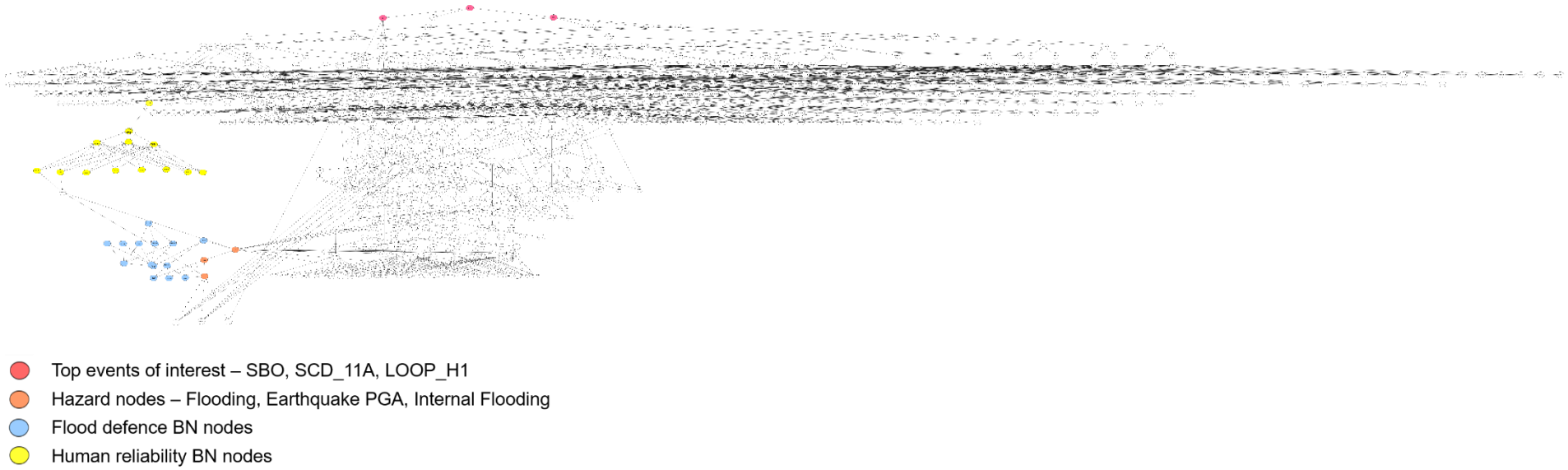

Figure 22: Unified BN integrating subnetworks for project accident scenario

(vectorised image can be accessed here – download file before viewing): https://drive.google.com/file/d/1jvdrN3mOGcCDt3iqRVac5bJJqxwPueYQ/view)

5.4 Results

Table 7 lists the marginal probabilities of the top event of the unified BN (LOOP_H1) as well as top events of each of the subnetworks within the unified BN. Also shown, are their marginal probabilities without consideration of hazards. The marginal probabilities are not too different, as expected as the hazard events are relatively rare. However, if they were to occur, there could be a significant rise in top event probabilities as already identified from hazard integration with the SBO BN (Figure 18).

Table 7: Marginal probabilities of occurrence of key events before and after multi-risk integration

Event	Marginal probability of occurrence	
	Before hazard & subnetwork integration	**With hazards integrated in unified BN**
SBO	2.73×10^{-4}	2.78×10^{-4}
SCD_11A	5.38×10^{-4}	5.46×10^{-4}
Dike failure	4.26×10^{-2}	4.59×10^{-2}
Operator fails to start and control EFWS	2.26×10^{-2}	2.33×10^{-2}
LOOP_H1	1.25×10^{-7}	1.32×10^{-7}

5.4.1 Sensitivity analysis

Sensitivity analysis can be performed in several ways using BNs including global sensitivity methods developed as part of the NARSIS project (Rohmer and Gehl, 2020). Herein, we simply use the diagnostic inference capabilities of the BN. Evidence of occurrence and non-occurrence of top event is provided to the BN and posterior probabilities of other events in the network are calculated using Bayesian inference. Response of top event probability, of the SBO BN, to multiple hazards was presented in Section 5.2.2. Hazard interaction was also assumed only for the SBO BN, flood defence BN and the human reliability BN. Hence, the focus here, is on the ability to link the top event of the SCD_11 BN (which includes the SBO BN) to the hazards, but also to extraneous subnetworks – the flood defence and human reliability BNs.

The variations in posterior distributions of HEP and flood defence failure nodes, based on evidence to top event, are shown in Figure 23. Overtopping failure probability is negligible due to the relatively very low probability of the flood level exceeding the height of the dike at the site. While piping failure is most likely as determined by the fragility functions, the probability of global stability failure of the dike undergoes the maximum change. This already provides a sense of which aspects of flood defence stability are likely to most affect the top event – a deduction that is easily possible because of the association of dike reliability parameters with accident states of the NPP, via the unified BN.

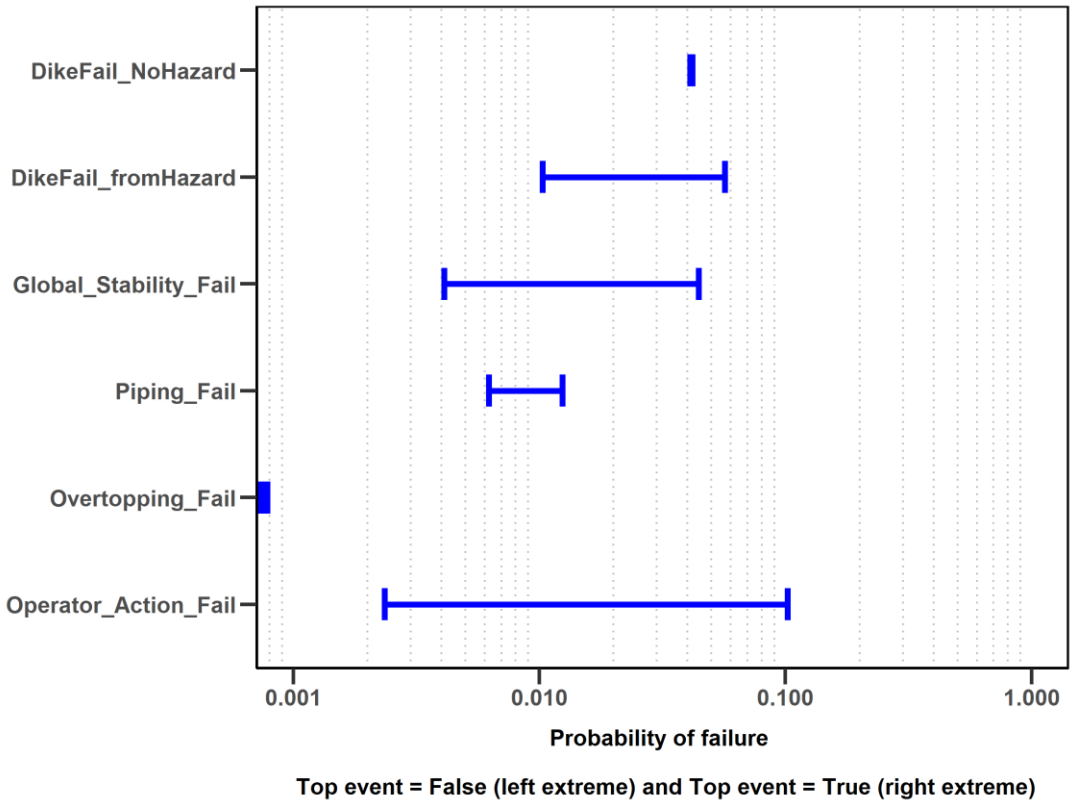

Figure 23: Posterior probability of flood defence nodes and operator error given evidence of non-occurrence and occurrence of LOOP_H1 (top event)

Figure 23 also shows that the posterior probability of human error changes by almost two orders of magnitude, indicating the significant influence of human reliability on plant safety, in this scenario. To further understand its impact on the top event, evidence of occurrence and non-occurrence of operator error was provided to the network to check the posterior probability of the top event. If operator error were to happen, the top event probability was calculated to be 1.57×10^{-7}, as compared to 6.61×10^{-7}, when the operator action was correctly performed – an increase of over 4 times while all other variables in the unified BN remained unchanged.

Figure 24 shows the sensitivity of HEP to various PSFs in the human subnetwork, prior to integration. Change in rating level from PSF R9 (relatively safe) to R1 (relatively unsafe) in the "Procedure" and "Experience/Training" PSFs has maximum impact over the probability of human error. Based on Section 5.3.4, "Available Time" and "Stressor" are the PSFs most impacted by hazard occurrence. With these facts as background, the posterior impact at the level of PSFs, to evidence of top event in the unified BN, is examined. Figure 25 shows the posterior probability distributions of the eight PSFs in the human reliability BN when evidence of non-occurrence (blue bars - safety) and occurrence (red bars - failure) of the top event (LOOP_H1) is provided to the unified BN. The change in probabilities of individual rating levels within PSFs is relatively minor. However, this change also manifest as a shift between rating levels – a degradation of PSFs as probability shifts from R9 (relatively safe) towards R1 (relatively unsafe). As a result, a significant change in HEP and top event probability is possible, even with a relatively minor change in the state of PSFs.

Thus, the unified BN clearly demonstrates the ability of the BN-based risk model to understand dependencies that are typically not considered in design or are not readily obtained from existing PSA tools. This is also possible because the top event is linked to various SSCs, including input parameters of their individual, BN-based reliability models.

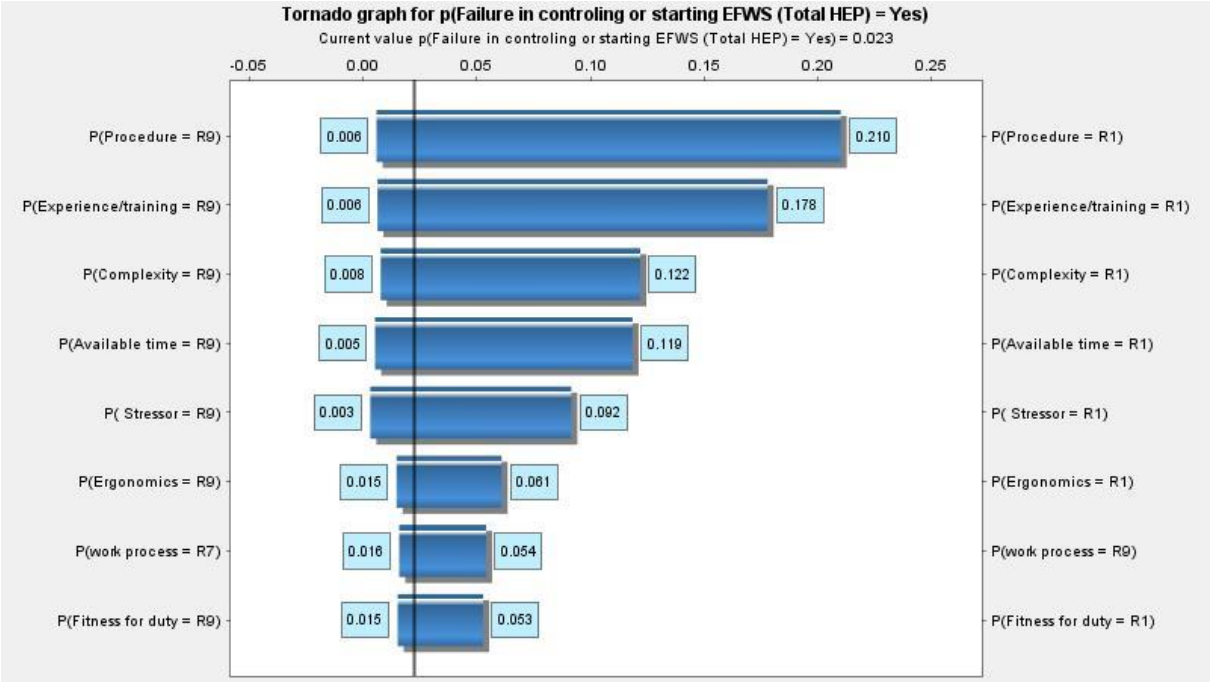

Figure 24: Sensitivity of HEP to different PSFs based on the human reliability subnetwork

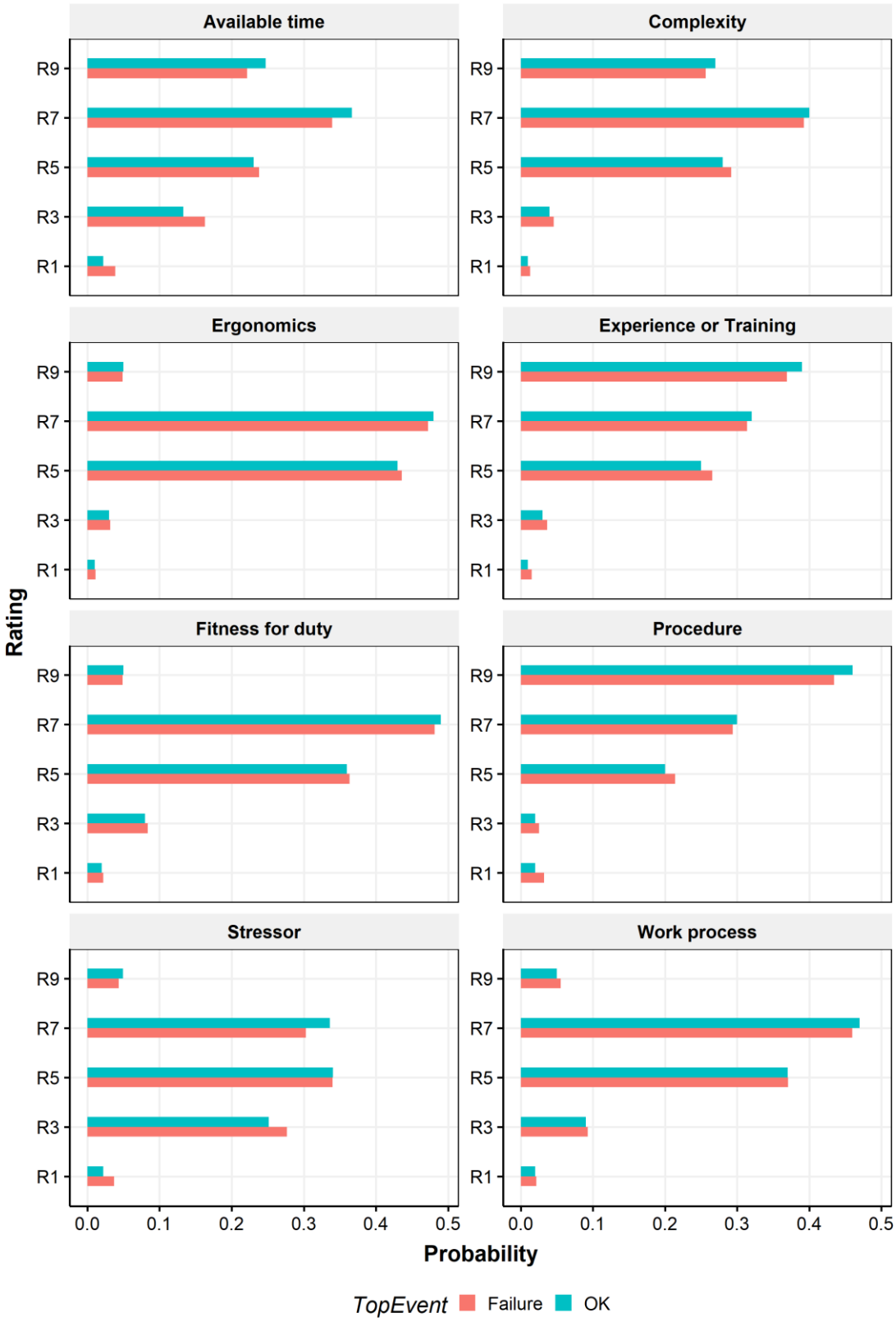

Figure 25: Posterior probability distributions of PSFs in the unified BN, given evidence of non-occurrence and occurrence of top event

5.5 Challenges

One significant challenge in the implementation of such unified BNs is the large computational load (run-time and/or memory used) due to discretised hazard nodes, detailed uncertainty representation of fragility parameters, continuous variables (such as in the flood defence BN) or large CPTs due to multi-state variables (such as in the human reliability BN). As a rule of thumb, representing continuous variables increases run-time while larger CPTs increase the file size of the model and its memory usage. The computational load on the network can potentially be eased using the iterative BN-based risk integration methodology described in Section 3.2. In the above described integration process for the project accident scenario, such removal of inconsequential hazards and dependencies were already done during hazard analysis (D1.6 – Daniell et al., 2019). Further, the filtering of less important hazard ranges based on fragility parameters was also performed separately. Despite such efforts, the unified BN approach is computationally more intensive as seen in Table 8.

For the SBO BN with hazards, two models were used – discretised and continuous calculation of damage states. In the discretised calculation, the CPTs at the damage state nodes are calculated externally and input to the node, whereas in the continuous calculation, fragility calculations are performed in the BN (as described in Section 3.3.2). While the discretised fragility calculation results in a similar run-time as the OOBN, the memory used is close to 4 times higher. On the other hand, when fragility calculations are performed using continuous nodes in the BN, the run-time increases close to 40 times, while the memory used remains almost the same when compared to the OOBN.

The unified BN for the project accident scenario – combining the SBO, SCD_11, flood defence and human reliability BNs – resulted in a significantly higher computational load. While the memory used increased linearly, the run-time was 44 times slower than the slowest individual subnetwork. Performing in-built sensitivity analysis on the desktop version of AgenaRisk® was impossible due to the large size of the unified BN model for the project accident scenario. Hence, plant-wide application of a unified BN risk model could encounter very high computational demands.

Table 8: Computation load for BNs in this study

Bayesian network reference	Run-time (seconds)	Maximum Memory used (MB)
SBO	~1	272
SBO with hazards – OOBN	~1	272
SBO with hazards – unified BN (discretised fragility calculations)	~1	1024
SBO with hazards – unified BN (continuous fragility calculations as in Section 3.3.2)	39	276
SCD_11	45	680
Flood defence	28	524
Human reliability	4	1088
Unified BN for project accident scenario	1980	3000

A solution to manage the computational requirements may be to combine the OOBN and unified BN approach to integration, where subnetworks are integrated only where necessary while other subnetworks remain as separate risk objects. This, of course, needs a thorough analysis of dependence across the various SSCs in the NPP and a judicious application of the BN method to maximise its advantages. Firstly, all the ET/FTs at an NPP may be converted to risk objects using the OOBN approach, to first reproduce the results of existing PSA. Next, subnetworks may be integrated using unified BNs as required. While this would not represent

a complete solution by modelling every dependence in the NPP, it would still complement and improve existing PSA results. Other minor, technical improvements include the use of divorcing of discrete nodes where possible. Also, much of the computational time often comes from the static discretisation of hazard nodes which impact several SSCs across the risk model. Reasonably accurate fitting of parametric distributions to hazard curves can avoid inefficient static discretisation of nodes, and instead, take advantage of dynamic discretisation of continuous nodes. Similarly, the use of non-parametric BNs can also significantly reduce the computational load of large BNs, with the necessary assumption of dependence between variables following the Gaussian copula (Morales-Nápoles and Steenbergen, 2015). In some cases, the diagnostic inference abilities in the OOBN approach may be improved by adopting methods as in Koller and Pfeffer (1997) or Neil et al. (2000). However, these methods are intended for encapsulation of variables within an object and the repeated use of model fragments in different contexts, both of which were not relevant to the example in this study.

Another challenge may be the large amount of time and workload involved in eliciting expert judgements regarding various probability distributions of variables. A significant and dedicated effort would be needed to transform existing PSA to BNs and improve it by eliciting expert judgements where needed. Again, the risk analyst must determine areas where there is value in such an exercise. The sensitivity results from the BN can be useful in this regard.

While computational demands are high for BNs, equivalent comparisons have not been made with existing PSA tools in this project. An accurate comparison would shed more light on the effectiveness of BNs in PSA in terms of computational feasibility.

5.6 Summary of findings

The general advantages and disadvantages of BNs as compared to FTs were discussed in detail deliverable D3.2 (Mohan et al., 2021) and D4.5 (Kaszko et al., 2021). Here, we summarise the findings from this study regarding the use of BNs for multi-risk integration.

- A stepwise, iterative multi-risk framework for risk integration using BNs was proposed. The methodology was applied to the project accident scenario of LOOP-induced SBO and SCD_11 events.
- Technical and human aspects were successfully integrated in a multi-hazard scenario using BNs. Multiple hazards, surrogate models for systems, human reliability methods and existing PSA information were all integrated under one risk framework, allowing for understanding of various dependencies.
- BNs can directly incorporate continuous random variables without the need for additional modifications as in the case of fault trees. Also, it is easy to integrate expert judgement in BNs. These advantages, demonstrated in the subnetworks, are also carried over into the unified BN.
- As more complex systems are modelled, with increased common cause effects, BNs can grow in size, making visualisation and computation challenging. Dependencies between components can become visually indecipherable.

5.6.1 Unified BN vs. OOBN

Utilising the advantages of BNs

- Diagnostic inference and Bayesian updating are inherent advantages of BNs. In OOBNs, these features are limited to within risk objects and cannot be performed across objects. Thus, unified BNs better preserve some key advantages of BNs over FTs.
- The unified integration of subnetworks with external hazards can help understand links between the top event of interest and various SSCs in the NPP, and reveal unforeseen dependencies. While using many hazard trees as in OOBNs, dependencies may be missed between different variables across scenarios. Using a unified BN could possibly limit such omissions.

Using existing PSA information

- ET and FTs in existing PSA can be equivalently modelled as OOBNs, allowing for easy transition with parallel application as opposed to the unified BN approach, where the logical interactions of event trees are housed in CPTs of hazard nodes. Hence, OOBNs can also be more easily implemented for plant-wide applications.

Computational load

- Multi-hazard integration under a unified BN, with several variables influenced by hazards and complex subnetworks, can result in significant computational challenges.
- One solution to manage the computational requirements may be to combine the OOBN and unified BN approach to integration, where subnetworks are integrated only where necessary while other subnetworks remain as separate risk objects.

5.7 Recommendations for further research

- Dynamic BNs is a type of BN that models relationships between variables over adjacent time steps (Jensen and Nielsen, 2007). Dynamic BNs were not considered in this study and must be explored as their use can provide significant improvements in PSA.
- The use of BNs in accident diagnosis and management should be explored further.
- Event/Fault trees and BNs can be implemented within the same software tool to allow for transition and parallel use, wherever possible.
- The disproportionately high number of discrete nodes in the BNs considered in this study meant non-parametric BNs were not chosen within this project. If extensive examination of all system events/variables can be done to represent most variables as continuous, non-parametric BNs, with necessary assumptions regarding the type of copula dependence, can be a more computationally efficient alternative (Hanea et al., 2015).
- Inference algorithms for object-oriented BNs can be improved to allow for diagnostic capabilities across BN objects, in a computationally feasible manner.
- While computational challenges were quoted as a challenge to BN implementation, an exact comparison with existing PSA tools was not possible in this project. An accurate comparison of computational time and cost will be valuable to the PSA practice.

6 References

Abrishami, S., Khakzad, N., Hosseini, S. M., & van Gelder, P. (2020). BN-SLIM: A Bayesian Network methodology for human reliability assessment based on Success Likelihood Index Method (SLIM). Reliability Engineering & System Safety, 193, 106647. doi:https://doi.org/10.1016/j.ress.2019.106647

Ale, B. J. M., Bellamy, L. J., Cooke, R. M., Goossens, L. H. J., Hale, A. R., Roelen, A. L. C., & Smith, E. (2006). Towards a causal model for air transport safety—an ongoing research project. Safety science, 44(8), 657-673. doi:https://doi.org/10.1016/j.ssci.2006.02.002

Andersen, V., Lee, L., Patel, P., & Burns, E. (2013). Seismic probabilistic risk assessment implementation guide (EPRI 3002000709).

Bachmann, D., Huber, N. P., Johann, G., & Schüttrumpf, H. (2013). Fragility curves in operational dike reliability assessment. Georisk: Assessment and Management of Risk for Engineered Systems and Geohazards, 7(1), 49-60. doi:10.1080/17499518.2013.767664

Bobbio, A., Portinale, L., Minichino, M., & Ciancamerla, E. (2001). Improving the analysis of dependable systems by mapping fault trees into Bayesian networks. Reliability Engineering & System Safety, 71(3), 249-260. doi:https://doi.org/10.1016/S0951-8320(00)00077-6

Bruneliere, H., Rastiello, G., Barry, T., Brandelet, J.-Y., Perrichon, L., Duflot, N., Guigeno, Y., Darnowski, P., Mazgaj, P., & Stepień, M. (2018). Definition of a simplified theoretical NPP representative of the European fleet (Technical Report D4.1). Retrieved from NARSIS project: Confidential deliverable

Cooke, R. (1991). Experts in uncertainty: opinion and subjective probability in science: Oxford University Press on Demand.

Cooke, R. M., & Goossens, L. L. H. J. (2008). TU Delft expert judgment data base. Reliability Engineering & System Safety, 93(5), 657-674. doi:https://doi.org/10.1016/j.ress.2007.03.005

Daniell, J., Schaefer, A., Wenzel, F., Hacker, E., & Edrich, A.-K. (2019). Development of single and secondary hazard assessment methodologies including uncertainty quantification and comparison - Characterization of potential physical threats due to different external hazards and scenarios (D1.6). Retrieved from http://www.narsis.eu/page/deliverables

Fenton, N. Transforming a continuous probability value into a Boolean. (2015). www.youtube.com/watch?v=5Yp9OsnK6Wk

Fenton, G., & Griffiths, D. V. (2008). Risk assessment in geotechnical engineering (Vol. 461): John Wiley & Sons, Inc.

Gehl, P., & Rohmer, J. (2018). Vector intensity measures for a more accurate reliability assessment of NPP sub-systems. Paper presented at the Technological Innovations in Nuclear Civil Engineering, France, Paris-Saclay.

Gehl, P., Seyedi, D. M., & Douglas, J. (2013). Vector-valued fragility functions for seismic risk evaluation. Bulletin of Earthquake Engineering, 11(2), 365-384. doi:10.1007/s10518-012-9402-7

Hanea, A. M., Morales Napoles, O., & Ababei, D. (2015). Non-parametric Bayesian networks: Improving theory and reviewing applications. *Reliability Engineering & System Safety, 144*, 265-284. doi:https://doi.org/10.1016/j.ress.2015.07.027

Hicks, M. A., & Samy, K. (2004). Stochastic evaluation of heterogeneous slope stability. Italian Geotechnical Journal, 38(2), 54-66.

Hofmann, D. A., Jacobs, R., & Landy, F. (1995). High reliability process industries: Individual, micro, and macro organizational influences on safety performance. Journal of Safety Research, 26(3), 131-149. doi:https://doi.org/10.1016/0022-4375(95)00011-E

Hopkins, A. (2011). Risk-management and rule-compliance: Decision-making in hazardous industries. Safety science, 49(2), 110-120. doi:https://doi.org/10.1016/j.ssci.2010.07.014

Janic, M. (2000). An assessment of risk and safety in civil aviation. Journal of Air Transport Management, 6(1), 43-50. doi:https://doi.org/10.1016/S0969-6997(99)00021-6

Jensen, F. V., & Nielsen, T. D. (2007). *Bayesian networks and decision graphs* (Vol. 2): Springer.

Kaszko, A. P., Slawomir, Mohan, V. K. D., Vardon, P.J.; Karanta, I. & Tyrväinen, T. (2021). Reactor safety analysis results useful for accident analysis, considering deterministic and probabilistic approaches; Comparison of new and existing methods for reactor safety analysis (Technical Report D4.5 Chapter 4). Retrieved from http://www.narsis.eu/page/deliverables

Kazemi, R., Mosleh, A., & Dierks, M. (2017). A Hybrid Methodology for Modeling Risk of Adverse Events in Complex Health-Care Settings. Risk Analysis, 37(3), 421-440.

Koller, D., & Friedman, N. (2009). Probabilistic graphical models: principles and techniques: MIT press.

Koller, D., & Pfeffer, A. (1997). Object-oriented Bayesian networks. Paper presented at the Proceedings of the Thirteenth conference on Uncertainty in artificial intelligence, Providence, Rhode Island.

Lees, F. (2005). 2 - Hazard, Incident and Loss. In S. Mannan (Ed.), Lees' Loss Prevention in the Process Industries (Third Edition) (pp. 2/1-2/27). Burlington: Butterworth-Heinemann.

Leveson, N., Dulac, N., Marais, K., & Carroll, J. (2009). Moving Beyond Normal Accidents and High Reliability Organizations: A Systems Approach to Safety in Complex Systems. Organization Studies, 30(2-3), 227-249. doi:10.1177/0170840608101478

Liu, Z., Nadim, F., Garcia-Aristizabal, A., Mignan, A., Fleming, K., & Luna, B. Q. (2015). A three-level framework for multi-risk assessment. Georisk: Assessment and Management of Risk for Engineered Systems and Geohazards, 9(2), 59-74. doi:10.1080/17499518.2015.1041989

Mignan, A., Wiemer, S., & Giardini, D. (2014). The quantification of low-probability–high-consequences events: part I. A generic multi-risk approach. Natural Hazards, 73(3), 1999-2022. doi:10.1007/s11069-014-1178-4

Mohaghegh, Z., Kazemi, R., & Mosleh, A. (2009). Incorporating organizational factors into Probabilistic Risk Assessment (PRA) of complex socio-technical systems: A hybrid technique formalization. Reliability Engineering & System Safety, 94(5), 1000-1018. doi:https://doi.org/10.1016/j.ress.2008.11.006

Mohan, V. K. D., Vardon, P. J., Dusic, M., van Gelder, P. H. A. J. M., Hicks, M. A., & Burgazzi, L. (2018). Risk integration methods for high risk industries (Technical Report D3.1). Retrieved from http://www.narsis.eu/page/deliverables

Mohan, V. K. D., Vardon, P. J., Hicks, M. A., & van Gelder, P. H. A. J. M. (2019). Uncertainty Tracking and Geotechnical Reliability Updating Using Bayesian Networks. Paper presented at the 7th International Symposium on Geotechnical Safety and Risk (ISGSR), Taipei, Taiwan.

Mohan, V. K. D., Vardon, P. J., van Gelder, P. H. A. J. M., Abrishami, S., Guldenmund, F., & Gehl, P. (2021). Development of risk sub-networks for technical and social/organisational aspects (Technical Report D3.2). Retrieved from http://www.narsis.eu/page/deliverables

Morales-Nápoles, O., & Steenbergen, R. D. J. M. (2015). Large-Scale Hybrid Bayesian Network for Traffic Load Modeling from Weigh-in-Motion System Data. Journal of Bridge Engineering, 20(1), 04014059. doi:doi:10.1061/(ASCE)BE.1943-5592.0000636

Neil, M., Fenton, N., & Nielson, L. (2000). Building large-scale Bayesian networks. The Knowledge Engineering Review, 15(3), 257-284.

Neil, M., Tailor, M., & Marquez, D. (2007). Inference in hybrid Bayesian networks using dynamic discretization. Statistics and Computing, 17(3), 219-233. doi:10.1007/s11222-007-9018-y

Pearl, J. (1988). Probabilistic Reasoning in Intelligent Systems. Networks of Plausible Inference. San Mateo: Morgan Kaufmann Publishers Inc. .

Rausand, M. (2013). Risk assessment: theory, methods, and applications (Vol. 115): John Wiley & Sons.

Roberts, K. H. (1990). Some Characteristics of One Type of High Reliability Organization. Organization Science, 1(2), 160-176. doi:10.1287/orsc.1.2.160

Rohmer, J., & Gehl, P. (2020). Sensitivity analysis of Bayesian networks to parameters of the conditional probability model using a Beta regression approach. Expert Systems with Applications, 145, 113130. doi:https://doi.org/10.1016/j.eswa.2019.113130

Tyagunov, S., Vorogushyn, S., Muñoz Jimenez, C., Parolai, S., & Fleming, K. (2018). Multi-hazard fragility analysis for fluvial dikes in earthquake-and flood-prone areas. Natural Hazards and Earth System Sciences, 18(9), 2345-2354.

US NRC. (1975). WASH 1400: Reactor safety study - An assessment of accident risks in U.S. commercial nuclear power plants. Washington DC: N.R.C.; National Technical Information Service {{URL: https://www.nrc.gov/reading-rm/doc-collections/nuregs/knowledge/km0010/}.

van Erp, N., & van Gelder, P. H. A. J. M. (2015). Risk Analysis framework for single and multiple hazards. Technical Report D5.1, RAIN Project (Risk Analysis of Infrastructure Networks in Response to Extreme Weather). Grant No. 608166. Retrieved from

Yerukala, R., & Boiroju, N. K. (2015). Approximations to standard normal distribution function. International Journal of Scientific & Engineering Research, 6(4), 515-518.